

Well-Posed KL-Regularized Control via Wasserstein and Kalman–Wasserstein KL Divergences

Viktor Stein *

Adwait Datar †

Nihat Ay †‡

February 3, 2026

Abstract

Kullback-Leibler divergence (KL) regularization is widely used in reinforcement learning, but it becomes infinite under support mismatch and can degenerate in low-noise limits. Utilizing a unified information-geometric framework, we introduce (Kalman)-Wasserstein-based KL analogues by replacing the Fisher-Rao geometry in the dynamical formulation of the KL with transport-based geometries, and we derive closed-form values for common distribution families. These divergences remain finite under support mismatch and yield a geometric interpretation of regularization heuristics used in Kalman ensemble methods. We demonstrate the utility of these divergences in KL-regularized optimal control. In the fully tractable setting of linear time-invariant systems with Gaussian process noise, the classical KL reduces to a quadratic control penalty that becomes singular as process noise vanishes. Our variants remove this singularity, yielding well-posed problems. On a double integrator and a cart-pole example, the resulting controls outperform KL-based regularization.

1 Introduction

The Kullback-Leibler (KL) divergence [32] between two probability measures $\mu, \nu \in \mathcal{P}(M)$,

$$\text{KL}(\mu \mid \nu) := \begin{cases} \int_M \ln\left(\frac{d\mu}{d\nu}\right) d\mu, & \text{if } \mu \ll \nu, \\ \infty, & \text{else} \end{cases} \quad (1)$$

can be interpreted dynamically and geometrically as a time-weighted kinetic energy along geodesics in the Fisher-Rao geometry on probability measures: if $\mu \ll \nu$, then

$$\text{KL}(\mu \mid \nu) = \int_0^1 t \|\dot{\gamma}(t)\|_{\gamma(t)}^2 dt, \quad (2)$$

where γ is the Fisher-Rao dual geodesic with respect to the mixture connection with $\gamma(0) = \nu$ and $\gamma(1) = \mu$.

*Institute of Mathematics, Technische Universität Berlin, Straße des 17. Juni 136, 10623 Berlin, Germany.
 stein@math.tu-berlin.de. <https://tu.berlin/imageanalysis>

†Institute for Data Science Foundations, Hamburg University of Technology, 21073 Hamburg, Germany.
 {adwait.datar,nihat.ay}@tuhh.de

‡Santa Fe Institute, Santa Fe, NM 87501, USA.

Replacing the prefactor t in the integral with its average, $\frac{1}{2}$, yields a symmetric quantity, namely the squared geodesic distance on the manifold of probability densities. If we replace the Fisher-Rao geometry by the Wasserstein-2 geometry, this geodesic distance becomes the well-known Wasserstein-2 distance from optimal transport [11, 59, 60].

A fundamental shortcoming of the KL is that it is not sensitive to the supports of the probability measures involved; for example, $\text{KL}(\delta_x \mid \delta_y) = \infty$ independently of the distance of x and y . On the other hand, the Wasserstein-2 distance fulfills $W_2(\delta_x, \delta_y) = \|x - y\|_2$. Motivated by this, in this paper, we **replace the Fisher-Rao geometry in (2) by Wasserstein-like geometries** and study the resulting divergence functionals, which we call *state-space-aware KL divergences*.

The Wasserstein geometry is widely popular in the machine learning community [2, 10, 16, 40, 47]. For example, the authors of [58] replace the KL-based objective in the variational autoencoder (VAE) by one based on the Wasserstein distance and report improved performance. Another choice would have been to replace the KL, an asymmetric quantity, with its Wasserstein analog, which is the guiding principle for our investigations.

KL regularization is ubiquitous in reinforcement learning and control, appearing in linearly-solvable and path-integral control formulations [30, 56, 57], in policy-search and trust-region methods [50], and more recently in optimal control and LQG/LQR-type settings [29]. However, it is well known that the KL divergence is sensitive to support mismatch and diverges as measures become increasingly concentrated, such as in low-noise or deterministic limits. To isolate and understand this behavior, we study divergence-regularized control in the fully tractable Linear Quadratic Regulator (LQR) setting. For linear time-invariant dynamics with Gaussian process noise, the classical KL reduces to a quadratic control penalty that becomes singular as the noise covariance vanishes, rendering the problem ill-posed in near-deterministic regimes. In contrast, our Wasserstein KL and Kalman-Wasserstein KL remain finite, interpolate between KL and transport-based penalties, and yield well-behaved optimal controls across both high- and low-noise regimes.

1.1 Prior work and contributions

We build on the work [6, 22], which introduced the canonical contrast function we study. In [5], this contrast function was studied in the context of the Wasserstein geometry, and the explicit values between Gaussians were calculated in [17].

As a first contribution, we establish a clear and rigorous connection between these geodesics and metric gradient flows of the arguably simplest functional on probability densities: the linear expectation function $\mu \mapsto \int f d\mu$. In PDE theory and mechanics, this is often called potential energy. Furthermore, the gradient flows of simple energies in more complicated geometries are explored in [28] and related to transformers.

Although in special cases our new formulas collapse to relatively simple ones (see, e.g. (10)), our approach provides a principled and geometric interpretation of frequently used ad hoc regularizations. They also show how, in a certain sense, the Kalman-Wasserstein geometry interpolates between the Fisher-Rao and the Wasserstein geometry.

Motivated by reinforcement learning, where KL regularization is ubiquitous, we study a model-based optimal control setting to clarify its theoretical role and show that our novel divergences serve as effective alternatives to KL, especially in the low-noise regime.

Notation The $n \times n$ identity matrix is denoted by I_n and the set of symmetric (positive definite) matrices by $\text{Sym}(\mathbb{R}; d)$ ($\text{Sym}_+(\mathbb{R}; d)$). We denote the time derivative by a dot, like $\dot{\varphi}_t$. The Lebesgue

measure is denoted by \mathcal{L} . For a Borel measurable map $f: X \rightarrow Y$ between metric spaces and a probability measure μ on X , its pushforward by f is a probability measure on Y , denoted by $f_{\#}\mu$ and defined by $(f_{\#}\mu)(A) := \mu(f^{-1}(A))$ for any measurable set $A \subset Y$. We set $\mathbb{E}_{\mu}[f] := \int_M f \, d\mu$. By grad we denote the Riemannian gradient and by div the Riemannian divergence with respect to the volume measure.

2 The Riemannian structure of the density manifold

In this section, we review the infinite-dimensional geometry of the space of positive smooth probability densities [9, 33]. We give examples like the Fisher-Rao or Wasserstein metric, define a particular notion of geodesics, and show how to obtain these geodesics by solving a gradient flow with respect to a linear functional.

The set of smooth positive probability densities on a compact n -dimensional Riemannian manifold $(M, \langle \cdot, \cdot \rangle)$ without boundaries equipped with its volume measure μ_g ,

$$P_+^\infty(M) := \left\{ \rho \in \mathcal{C}^\infty(M) : \rho > 0, \int_M \rho \, d\mu_g = 1 \right\},$$

with the tangent space at $\mu \in P_+^\infty(M)$ being

$$\begin{aligned} T_\mu P_+^\infty(M) &= \mathcal{S}_0^\infty(M) \\ &:= \{ \xi = f\mu_g : f \in \mathcal{C}^\infty(M), \xi(M) = 0 \}, \end{aligned}$$

and the cotangent space defined as

$$T_\mu^* P_+^\infty(M) := \mathcal{C}^\infty(M)/\mathbb{R},$$

is a smooth infinite-dimensional Fréchet manifold. We set $S^\infty(M) := \{f\mu_g : f \in \mathcal{C}^\infty(M)\}$.

As in [8], we construct Riemannian metrics on $P_+^\infty(M)$ using inertia operators.

Definition 2.1 (Inertia operator). A *inertia operator* (or lowering of indices / musical isomorphism, or *Onsager* operator [36]) is a $L^2(M; \mu_g)$ -selfadjoint and positive definite operator

$$\varphi_\mu^G: \mathcal{C}^\infty(M)/\mathbb{R} \rightarrow \mathcal{S}_0^\infty(M)$$

for $\mu \in P_+^\infty(M)$, where G will denote the geometry, i.e., Wasserstein or Fisher-Rao. \diamond

As in [61], we can write a Riemannian metric on $P_+^\infty(M)$ associated to φ_μ^G either in terms of tangent vectors $a, b \in \mathcal{S}_0^\infty(M)$ or in terms of covectors of equivalence classes $[f], [g] \in \mathcal{C}^\infty(M)/\mathbb{R}$. They are related by $\varphi_\mu^G([f]) = a$ and $\varphi_\mu^G([g]) = b$.

Definition 2.2 (Regular Riemannian metric on $P_+^\infty(M)$). The Riemannian metric associated with φ_μ^G is

$$g_\mu^G(a, b) := \langle a, (\Psi_\mu \circ (\varphi_\mu^G)^{-1})(b) \rangle_{L^2(M; \mu_g)} = \langle \varphi_\mu^G([f]) \cdot \Psi_\mu([g]) \rangle_{L^2(M; \mu_g)} =: \langle [f], [g] \rangle_\mu^G,$$

where $\Psi_\mu: \mathcal{C}^\infty(M)/\mathbb{R} \rightarrow \mathcal{C}_0^\infty(M, \mu)$, $[f] \mapsto f - \mathbb{E}_\mu[f]$ and

$$C_0^\infty(M; \mu) := \left\{ f \in \mathcal{C}^\infty(M) : \int_M f \, d\mu = 0 \right\}.$$

The *density manifold* $P_+^\infty(M)$ equipped with this metric is denoted by $(P_+^\infty(M), g^G)$. \diamond

We now detail examples of Riemannian metrics on $P_+^\infty(M)$.

Example 2.3 (Fisher-Rao metric). Let $\mu \in P_+^\infty(M)$. The Fisher-Rao inertia operator is

$$\varphi_\mu^{\text{FR}}: \mathcal{C}^\infty(M)/\mathbb{R} \rightarrow \mathcal{S}_0^\infty(M), \quad [f] \mapsto (f - \mathbb{E}_\mu[f])\mu.$$

Since the inverse of φ_μ^{FR} has a closed form, we can write the metric as

$$g_\mu^{\text{FR}}(a, b) := \int_M \frac{da}{d\mu} \cdot \frac{db}{d\mu} d\mu.$$

The sectional curvature of $(P_+^\infty(M), g^{\text{FR}})$ is $\equiv \frac{1}{4}$ [24]. •

Example 2.4 (Otto's Wasserstein metric with non-linear mobility). The Otto isomorphism [44, 59, 60] is given by the weighted Laplacian

$$\varphi_\mu^{\text{O}}: \mathcal{C}^\infty(M)/\mathbb{R} \rightarrow \mathcal{S}_0^\infty(M), \quad [f] \mapsto -\text{div}_\mu(\text{grad}(f))\mu,$$

where div_μ is explained in [5, Sec. 3]. The associated cotangent inner product is given by (using integration by parts)

$$\langle\langle [f], [g] \rangle\rangle_\mu^{\text{O}} := \int_M \langle \text{grad}(f), \text{grad}(g) \rangle d\mu.$$

The curvature, Levi-Civita connection, and more of $(P_+^\infty(M), g^{\text{O}})$ is extensively discussed in [41].

If $m: [0, \infty) \rightarrow [0, \infty)$ is a so-called *mobility function* [34, Sec. 2.3] [19, Rem. 12], which models conductivity/permeability of the transport process, then we can describe the Wasserstein-2 metric with nonlinear mobility [15, 18] using

$$\varphi_\mu^{O_m}: \mathcal{C}^\infty(M)/\mathbb{R} \rightarrow \mathcal{S}_0^\infty(M), \quad [f] \mapsto -\text{div} \left(m \left(\frac{d\mu}{d\mu_g} \right) \text{grad}(f) \right), \quad (3)$$

with associated cotangent inner product

$$\langle\langle [f], [g] \rangle\rangle_\mu^{O_m} := \int_M \left\langle \text{grad}(f), m \left(\frac{d\mu}{d\mu_g} \right) \text{grad}(g) \right\rangle d\mu_g.$$

The Levi-Civita connection and the curvature of (P_+^∞, g^{O_m}) for $M = \mathbb{R}$ has been investigated in [35].

A particular instance is the Kalman-Wasserstein metric g^{KW} [25] with mobility $m_\lambda(f) := f(C(f) + \lambda \text{id}_{TM})$, where $C(f)$ is the Riemannian covariance¹ of the density f , see [1, Defn. 3.2], and $\lambda > 0$ is some regularization parameter.

For the constant mobility $m \equiv 1$ we recover a flat \dot{H}^{-1} (“linearized Wasserstein” [46]) structure $g^{\dot{H}^{-1}}$. •

2.1 Metric gradient flows on the density manifold

Consider a functional $E: P_+^\infty(M) \rightarrow \mathbb{R}$. First, we define the covector field δE on $P_+^\infty(M)$, induced by the ambient Fréchet space $\mathcal{C}^\infty(M)$. We can then conveniently express the Riemannian gradient $\text{grad}(E)$, which is a tangent vector field, as $\varphi_\mu[\delta E(\mu)]$, recovering the familiar formula $g(\text{grad}(E), s) = \langle\langle \delta E, s \rangle\rangle$ for any vector field s on $P_+^\infty(M)$.

¹For it to be well-defined, we require that on M , the 2-Fréchet mean is unique [1, Subsec. 2.2], which holds, e.g., for Hadamard manifolds [45].

Definition 2.5 (Linear functional derivative). The *first variation* (or: linear functional derivative) of E , if it exists, is the one-form $\delta E: P_+^\infty(M) \rightarrow \mathcal{C}_0^\infty(M; \mu)$ fulfilling

$$\langle \delta E(\mu), \sigma \rangle_{L^2(M, \mu_g)} = \frac{d}{dt} E(\mu + t\sigma) \Big|_{t=0} \quad \forall \mu \in P_+^\infty(M)$$

for all $\sigma \in \mathcal{S}_0^\infty(M)$ such that $\mu + t\sigma \in P_+^\infty(M)$ for all sufficiently small $t \in \mathbb{R}$. ◇

For some examples of functional derivatives of common functionals, see [51, Tab. 1].

Note that, in the following definition, we follow a different sign convention than [5].

Definition 2.6 (Metric gradient flow on $P_+^\infty(M)$). We say that a smooth curve $\mu: [0, \infty) \rightarrow P_+^\infty(M)$, $t \mapsto \mu_t$ is a $(P_+^\infty(M), G)$ -gradient flow of a functional $E: P_+^\infty(M) \rightarrow \mathbb{R}$ starting at $\mu(0)$ if

$$\partial_t \mu_t = -\text{grad}_\mu^G(E)(\mu_t) =: -\varphi_{\mu_t}^G[\delta E(\mu_t)] \quad t > 0. \quad \diamond$$

We now generalize [5, Thm. 1].

Proposition 2.7 (Metric gradients of the expectation functional). For $f \in \mathcal{C}^\infty(M)$, we have

$$\text{grad}_\mu^G \mathbb{E}[f] = \varphi_\mu^G([f]).$$

This property uniquely characterizes these metrics.

Proof. For $F(\mu) := \mathbb{E}_\mu[f]$ we have $\delta F(\mu) = [f]$. The uniqueness follows exactly as in [5, Prop. 3]. □

2.2 Dual geodesics on the density manifold

We now generalize the construction in [22], and define, analogously to [5, Eq. (33)] the *G-parallel transport*.

Definition 2.8 (*G*-parallel transport). The *G-parallel transport* from $\mu \in P_+^\infty(M)$ to $\nu \in P_+^\infty(M)$ is

$$\Pi_{\mu, \nu}^G: T_\mu P_+^\infty(M) \rightarrow T_\nu P_+^\infty(M), \quad (\mu, a) \mapsto (\nu, (\varphi_\nu^G \circ (\varphi_\mu^G)^{-1})(a)). \diamond$$

Then, by construction of g^G and Π^G , the resulting *G connection* $\nabla^{(G)}$ is dual to the mixture connection $\nabla^{(m)}$ [7] in the sense of [5, Eq. (29)].

The geodesic γ , which is *G*-dual with respect to $\nabla^{(m)}$, or simply, the *G-dual geodesic* satisfying $\gamma(0) = \mu$ and $\dot{\gamma}(0) = a$ is

$$\dot{\gamma}(t) = \varphi_{\gamma(t)}^G((\varphi_\mu^G)^{-1}(a)), \quad t \in \mathbb{R}.$$

We now make a precise connection between *G*-dual geodesics and the metric gradient flow of the expectation functional.

Theorem 2.9 (Characterizing *G*-dual geodesics). Let $\mu \in P_+^\infty(M)$ and $a \in \mathcal{S}_0^\infty(M)$. For any $f \in \mathcal{C}^\infty(M)$ with $a = \varphi_\mu^G([f])$, the *G*-dual geodesic satisfying $\gamma(0) = \mu$ and $\dot{\gamma}(0) = a$ is the *G*-gradient flow of the potential energy

$$\mathcal{F}: P_+^\infty(M) \rightarrow \mathbb{R}, \quad \mu \mapsto -\mathbb{E}_\mu[f].$$

3 state-space-aware KL-divergences

Taking inspiration from [22], we can now define new divergences using the canonical contrast function and the notion of geodesics defined above.

Definition 3.1 (G -divergence). The G -divergence is

$$D^G: P_+^\infty(M) \times P_+^\infty(M) \rightarrow [0, \infty],$$

$$(\mu \mid \nu) \mapsto \inf \left\{ \int_0^1 t g_{\gamma(t)}^G(\dot{\gamma}(t), \dot{\gamma}(t)) dt : \begin{array}{l} \gamma: [0, 1] \rightarrow P_+^\infty(M) \\ \text{is a } G\text{-dual geodesic,} \\ \gamma(0) = \mu, \gamma(1) = \nu \end{array} \right\}.$$

◊

Example 3.2. For $G = \text{FR}$ we obtain the reverse KL divergence, see theorem 4.9. For $G = \text{O}$ we obtain the WKL divergence from [17], see theorem 4.10. •

Remark 3.3 (Energy dissipation interpretation). By theorem 2.9, the *dissipation of \mathcal{F} along $\gamma(t)$* is

$$\begin{aligned} \frac{d}{dt} \mathcal{F}(\gamma(t)) &= -\langle \delta \mathcal{F}(\gamma(t)), \dot{\gamma}(t) \rangle_{L^2(M; \mu_g)} = -\langle \delta \mathcal{F}(\gamma(t)), \varphi_{\gamma(t)}^G([f]) \rangle_{L^2(M; \mu_g)} \\ &= - \int_M \dot{\gamma}(t) \Psi_{\gamma(t)}((\varphi_\mu^G)^{-1}(\dot{\gamma}(t))) d\mu_g \\ &= -g_{\gamma(t)}^G(\dot{\gamma}(t), \dot{\gamma}(t)) \leq 0. \end{aligned}$$

Hence, if there is a unique G -dual geodesic between μ and ν , then the G -divergence between μ and ν can be conveniently expressed as

$$D^G(\mu \mid \nu) = \int_0^1 t \left(-\frac{d}{dt} \mathcal{F}(\gamma(t)) \right) dt = \int_0^1 \mathcal{F}(\gamma(t)) dt - \mathcal{F}(\nu).$$

4 Explicit expressions for the state-space-aware KL divergence

In the following, we will consider the manifold $M = \mathbb{R}^d$, which is *non-compact* (see the discussion [33, pp. 730–731]). We will use the analogies of the formulas above, not claiming their well-definedness.

First, we will treat the linearized Wasserstein metric O_m with $m \equiv 1$. Since the linearized Wasserstein geometry is flat, the associated canonical divergence is a symmetric quantity resembling a squared norm.

Theorem 4.1 (Linearized Wasserstein KL-divergence = Coulomb MMD). *For $\mu, \nu \in P_+^\infty(\mathbb{R}^d)$, the linearized Wasserstein divergence $D^{\dot{H}^{-1}}(\mu \mid \nu)$ is equal to*

$$\frac{3}{2} \int_{\mathbb{R}^d} \int_{\mathbb{R}^d} \Phi(x - y) d(\mu - \nu)(x) d(\mu - \nu)(y), \quad (4)$$

where Φ is the fundamental solution of $-\Delta \Phi = \delta_0$.

Proof. See section A.1. □

Remark 4.2 (Wasserstein gradient flows of $D^{\dot{H}^{-1}}(\cdot | \nu)$). Up to the prefactor, the \dot{H}^{-1} divergence (4) is the so-called maximum mean discrepancy [13, 27] with the translation-invariant kernel $K(x, y) := \Phi(x - y)$. In the Fourier domain, it can be written as $(2\pi)^{-d} \int_{\mathbb{R}^d} \|\hat{\mu}(\xi) - \hat{\nu}(\xi)\|_2^2 \|\xi\|_2^{-2} d\xi$. For $d = 1$, the kernel is $K(x, y) = -\frac{1}{2}|x - y|$ and the (regularized) Wasserstein gradient flow of $D^{\dot{H}^{-1}}$ is treated in [20, 21]. For higher dimensions, Φ is related to the Coulomb kernel, and [14] discusses the Wasserstein gradient flow of $D^{\dot{H}^{-1}}$.

4.1 The state-space-aware KL divergence between elliptic distributions

First, we recall the higher-dimensional analog of scale-location families to higher dimensions, namely, elliptic distributions [49, Sec. 5]. They are essentially all the distributions that are invariant under the pushforward by affine linear functions.

Elliptic distributions

Definition 4.3 (Elliptic distribution). A probability distribution μ on \mathbb{R}^d is called *elliptic* if there exist $m \in \mathbb{R}^d$, $\Sigma \in \text{Sym}_+(\mathbb{R}; d)$ and a smooth, integrable function $g: [0, \infty) \rightarrow (0, \infty)$ with

- $\frac{\pi^{\frac{d}{2}}}{\Gamma(\frac{d}{2})} \int_0^\infty r^{\frac{d}{2}-1} g(r) dr = 1$ (normalization),
- $\int_0^\infty r^{\frac{d-1}{2}} g(r) dr < \infty$ (finite expectation),
- $\int_0^\infty r^{\frac{d}{2}} g(r) dr < \infty$ (finite variance),

such that its density is given by

$$p_{m, \Sigma, g} := \det(\Sigma)^{-\frac{1}{2}} g((\cdot - m)^\top \Sigma^{-1} (\cdot - m)).$$

Then, we write $\mu \sim E(m, \Sigma, g)$. ◊

Remark 4.4 (Affine pushforward of elliptic distribution). Given the affine linear map $f(x) := Ax + b$ for some $A \in \mathbb{R}^{d \times d}$ and $b \in \mathbb{R}^d$, we have that $\mu \sim E(m, \Sigma, g)$ implies that $f_\# \mu \sim E(Am + b, A\Sigma A^\top, g)$ [23, p. 279].

Example 4.5 (Elliptic distributions). For $g(x) = (2\pi)^{-\frac{d}{2}} e^{-\frac{1}{2}x}$ we obtain *Gaussian distributions* and for $g(x) = \frac{\Gamma(\frac{v+d}{2})}{\Gamma(\frac{v}{2})} (v\pi)^{-\frac{d}{2}} (1 + \frac{1}{v}x)^{-\frac{v+d}{2}}$ we obtain *student's t distributions* with parameter $v > 2$. There are also other less-known examples such as logistic distributions, power-exponential distributions for even parameters $p \in 2\mathbb{N}$, and generalized hyperbolic distributions, see [49, Sec. 6]. •

Remark 4.6. By lemma B.1, for $X \sim E(m, \Sigma, g)$ we have $\mathbb{E}[X] = m$ and $\mathbb{V}[X] = \kappa_g \Sigma$, where $\kappa_g := \frac{1}{d} \int_{\mathbb{R}^d} \|y\|^2 g(\|y\|^2) dy$. For Gaussian distributions, we have $\kappa_g = 1$ and for student's t with v degrees of freedom, we have $\kappa_g = \frac{v}{v-2}$.

Quadratic potentials We will see that for some of the metrics discussed above, we can choose the quadratic potential function $f(x) = \frac{1}{2}x^T Bx + b^T x + c$, where $b \in \mathbb{R}^d$ and we can without loss of generality choose $B \in \text{Sym}(\mathbb{R}; d)$ and $c = 0$, to obtain a geodesic from μ to ν , which stays in the submanifold of $E(\cdot, \cdot, g)$ distributions. We will find a closed-form expression for the gradient flow starting at μ and determine B and b from μ and ν .

Except for the Fisher-Rao metric, all metrics discussed above have the *divergence form*

$$\varphi_{\rho, \mathcal{L}}^G([f]) = -\nabla \cdot (\rho \cdot v^G(\rho, \nabla f)) \mathcal{L} \quad (5)$$

for some *velocity field* $v^G: P_+^\infty(M) \times \mathcal{C}^\infty(M) \rightarrow \mathcal{C}^\infty(M)$.

Example 4.7 (Affine vector fields for elliptic distributions). For $\lambda > 0$, we have

$$v^{\text{KW}}(p_{m, \Sigma, g}, \nabla f) = x \mapsto (\kappa_g \Sigma + \lambda I_d)(Bx + b), \quad (6)$$

as is verified in section B.1. Similarly, $v^{\text{O}}(\mu, \nabla f) = \nabla f$. All vector fields are affine linear functions. \bullet

Lemma 4.8 (Elliptic closure for affine linear vector fields). *Suppose $\dot{\rho}_t = -\nabla \cdot (\rho_t v_t)$ for an affine vector field $v_t(x) := S_t x + s_t$ smoothly varying in t , with $S_t \in \text{Sym}(\mathbb{R}; d)$ and $s_t \in \mathbb{R}^d$ for all $t \geq 0$. Then, we have closure in the family of elliptic distributions: if $\rho_0 \sim E(m_0, \Sigma_0, g)$, then $\rho_t \sim E(m_t, \Sigma_t, g)$, where (m_t, Σ_t) solves*

$$\begin{cases} \dot{m}_t = S_t m_t + s_t, \\ \dot{\Sigma}_t = S_t \Sigma_t + \Sigma_t S_t =: 2 \text{Sym}(S_t \Sigma_t). \end{cases} \quad (7)$$

Proof. See section A.2. \square

We will obtain explicit solutions of the system (7). Thus, by (4) and lemma B.2 we can then evaluate the divergence as

$$D^G(\mu \mid \nu) = \frac{\kappa_g}{2} \text{tr}(B\Sigma_1) + \frac{1}{2} m_1^T (Bm_1 + 2b) - \int_0^1 \frac{\kappa_g}{2} \text{tr}(B\Sigma_t) + \frac{1}{2} m_t^T (Bm_t + 2b) dt. \quad (8)$$

First, we recall the following well-known result.

Theorem 4.9 (D^{FR} = reverse KL). *For $\mu, \nu \in P_+^\infty(\mathbb{R}^d)$ with (24) we have $D^{\text{FR}}(\mu, \nu) = \text{KL}(\nu \mid \mu)$.*

Proof. See section B.2. \square

The following result provides a closed-form expression for the WKL divergence between two elliptic distributions and is a trivial extension of the result for Gaussian distributions developed in [17].

Theorem 4.10 (WKL divergence). *Let $\mu \sim E(m_0, \Sigma_0, g)$ and $\nu \sim E(m_1, \Sigma_1, g)$ and set $\Delta m = m_1 - m_0$. Then*

$$D^{\text{WKL}}(\mu \mid \nu) = \frac{\kappa_g}{4} \text{tr}(\Sigma_0 - \Sigma_1 + \Sigma_0 R^2 \log(R^2)) + \frac{1}{4} \left\| \sqrt{Q + 2 \log(R)^\perp} \Delta m \right\|^2, \quad (9)$$

where

$$R = \Sigma_0^{-\frac{1}{2}} \left(\Sigma_0^{\frac{1}{2}} \Sigma_1 \Sigma_0^{\frac{1}{2}} \right)^{\frac{1}{2}} \Sigma_0^{-\frac{1}{2}}$$

$$Q = (R - I)^\dagger (\log(R^2) R^2 - R^2 + I) (R - I)^\dagger.$$

Furthermore, if $\Sigma_0 \Sigma_1 = \Sigma_1 \Sigma_0$, then we get the following simplification:

$$D^{\text{WKL}}(\mu | \nu) = \frac{\kappa_g}{4} \left\| \sqrt{Q} \left(\sqrt{\Sigma_1} - \sqrt{\Sigma_0} \right) \right\|_F^2 + \frac{1}{4} \left\| \sqrt{Q + 2 \log(R)^\perp} \Delta m \right\|^2.$$

Proof. See Section A.3. \square

Theorem 4.11 (KWKL divergence). *Let $\mu \sim E(m_0, \Sigma_0, g)$ and $\nu \sim E(m_1, \Sigma_1, g)$, where Σ_0 and Σ_1 are simultaneously diagonalizable with eigenvalues $(s_0)_i$ and $(s_1)_i$. Set $\Delta m := m_1 - m_0$ and $\Delta \Sigma := \Sigma_1 - \Sigma_0$. If $\lambda < \frac{\kappa_g (s_0)_i (s_1)_i}{(s_1)_i - (s_0)_i}$ for all $i \in \{1, \dots, d\}$, with $(s_0)_i \neq (s_1)_i$, then*

$$D^{\text{KW}}(\mu | \nu) = \frac{\kappa_g}{4\lambda} \text{tr}(\Xi) + \frac{1}{2} \Delta m^\top \left(\Delta \Sigma^\perp \Sigma_{0,\lambda}^{-1} \Delta \Sigma^\perp + \frac{1}{2\lambda} P \Xi P (\sqrt{\Sigma_1} - \sqrt{\Sigma_0})^{-2} \right) \Delta m,$$

where $P := \Delta \Sigma (\Delta \Sigma)^\dagger = I - \Delta \Sigma^\perp$ and $\Sigma_{\ell,\lambda} := \kappa_g \Sigma_\ell + \lambda I$ for $\ell \in \{0, 1\}$, and

$$\Xi := \left(\Sigma_1 \ln(\Sigma_1 \Sigma_0^{-1}) + \frac{1}{\kappa_g} \Sigma_{1,\lambda} \ln(\Sigma_{0,\lambda} \Sigma_{1,\lambda}^{-1}) \right).$$

Proof. See section A.4. \square

Thus, for elliptic distributions with equal variance, taking KW-geodesics in the dynamical formulation of the KL (2) corresponds to the “ad-hoc numerical technique called [additive] covariance inflation” [55] (also called *enforcing a noise floor*) often used in the Kalman filter literature.

Corollary 4.12 (D^{KW} enforces a noise floor). *If $\mu \sim E(m_0, \Sigma, g)$ and $\nu \sim E(m_1, \Sigma, g)$, then*

$$D^{\text{KW}}(\mu | \nu) = \frac{1}{2} (\Delta m)^\top (\kappa_g \Sigma + \lambda I)^{-1} \Delta m. \quad (10)$$

In particular, for $\mu \sim \mathcal{N}(m_0, \Sigma)$ and $\nu \sim \mathcal{N}(m_1, \Sigma)$

$$D^{\text{KW}}(\mu | \nu) = \text{KL}(\mathcal{N}(m_0, \Sigma + \lambda I), \mathcal{N}(m_1, \Sigma + \lambda I)).$$

In particular, if Σ degenerates, then D^{KW} is still well-defined, unlike KL.

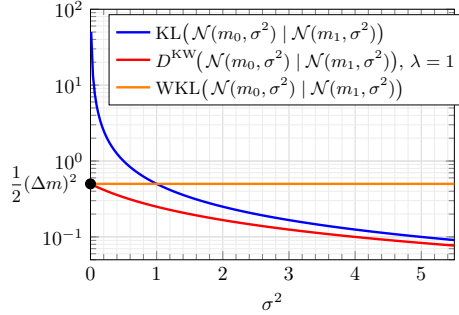


Figure 1: For $\mu \sim \mathcal{N}(m_0, \sigma^2)$ and $\nu \sim \mathcal{N}(m_1, \sigma^2)$, we compare $D^{\text{KW}}(\mu | \nu) = \frac{1}{2(\sigma^2 + \lambda)}(\Delta m)^2$ with $\text{KL}(\mu | \nu) = \frac{1}{2\sigma^2}(\Delta m)^2$ and $\text{WKL}(\mu | \nu) = \frac{1}{2}(\Delta m)^2$, where $\lambda = 1$ and $(\Delta m)^2 = \frac{1}{4}$.

Remark 4.13 (D^{KW} interpolates between KL and WKL). In Figure 1 we observe that D^{KW} is a smoothing of KL, since $\lim_{\lambda \searrow 0} D^{\text{KW}} = \text{KL}$. For $\lambda = 1$ we observe that D^{KW} interpolates between WKL and KL, since then

$$\lim_{\sigma^2 \rightarrow \infty} \frac{D^{\text{KW}}(\mu | \nu)}{\text{KL}(\mu | \nu)} = 1 = \lim_{\sigma^2 \searrow 0} \frac{D^{\text{KW}}(\mu | \nu)}{\text{WKL}(\mu | \nu)}.$$

On the other hand, D^{KW} is non-local.

5 Optimal Control Problems with Divergence-Based Regularization

In this section, we illustrate how the proposed Wasserstein-based KL analogues (WKL and KWKL) can serve as regularizers in stochastic linear–quadratic control. Classical KL-regularized formulations impose a quadratic control cost proportional to the inverse process noise covariance, which becomes singular as the noise vanishes. In contrast, the WKL- and KWKL-based penalties remain finite in this regime, yielding well-posed control problems and recovering meaningful limiting behaviors (see Corollary 5.1).

Consider linear time-invariant dynamics described by

$$x_{t+1} = Ax_t + Bu_t + w_t, \quad t \in \mathbb{N}, \quad (11)$$

where $x_t \in \mathbb{R}^n$ denotes the state, $u_t \in \mathbb{R}^m$ denotes the control input and $w_t \in \mathbb{R}^n$ denotes the process noise. Let $x_0 \sim \mathcal{N}(0, \Sigma_0)$ and assume the process noise w_t consists of independent and identically distributed random variables distributed² according to $\mathcal{N}(0, \Sigma_w)$. We restrict attention to linear feedback policies $u_t = Fx_t$ and want to find the optimal gain matrix F by minimizing the infinite-horizon discounted quadratic state cost

$$J(F) = \mathbb{E}_{w_t \sim \mathcal{N}(0, \Sigma_w)} \left[\sum_{t=0}^{\infty} \frac{1}{2} \gamma^t x_t^T Q x_t \right],$$

²As demonstrated in the preceding sections, we could instead choose $w_t \sim E(0, \Sigma_w, g)$ and everything works analogously.

with *discount factor* $\gamma \in (0, 1)$ and a user-specified $Q \in \text{Sym}_+(\mathbb{R}; d)$. To regularize control effort, we penalize deviations between the controller and and uncontrolled conditional state-transition distributions. Specifically, we add a divergence-based regularization term comparing

$$\begin{aligned} p_t &:= p(x_{t+1} | x_t, u_t) = \mathcal{N}(Ax_t + Bu_t, \Sigma_w), \\ p_0 &:= p(x_{t+1} | x_t, u_t = 0) = \mathcal{N}(Ax_t, \Sigma_w). \end{aligned}$$

Computing the divergences yields

$$\begin{aligned} D^{\text{KL}}(p_t | p_0) &= \frac{1}{2} u_t^\top B^\top \Sigma_w^{-1} B u_t, \\ D^{\text{WKL}}(p_t | p_0) &= \frac{1}{2} u_t^\top B^\top B u_t = \frac{1}{2} W_2(p_t, p_0)^2, \\ D^{\text{KW}}(p_t | p_0) &= \frac{1}{2} u_t^\top B^\top (\Sigma_w + \lambda I)^{-1} B u_t, \end{aligned}$$

where W_2 is the 2-Wasserstein distance. The KL-based regularizer explicitly depends on Σ_w^{-1} and thus diverges as Σ_w approaches singularity. In contrast, the KWKL-based and the WKL-based regularizers remain well-defined in this limit. With these regularization terms added to the state cost, the total cost with divergence-based regularization is

$$J^\circ(F) = \mathbb{E}_{w_t \sim \mathcal{N}(0, \Sigma_w)} \left[\sum_{t=0}^{\infty} \frac{\gamma^t}{2} (x_t^\top Q x_t + D^\circ(p_t | p_0)) \right],$$

where $\circ \in \{\text{KL, WKL, KW}\}$. Since the divergence contributes an additive quadratic term in u_t , each formulation reduces to a discounted LQR problem with effective control penalties (12). The problems $\arg \min_F J^\circ(F)$ possess closed-form solutions in the form of solutions to Riccati equations (see Appendix C).

As a consequence of Theorem C.1, we obtain:

Corollary 5.1 (Optimal policies). *Consider the LTI system (11) where (A, B) is stabilizable, $(A, Q^{1/2})$ is detectable, and B has full column rank. Let*

$$\begin{aligned} R_{\text{KL}} &= B^\top \Sigma_w^{-1} B, & R_{\text{WKL}} &= B^\top B, \\ R_{\text{KW}} &= B^\top (\Sigma_w + \lambda I)^{-1} B, \end{aligned} \tag{12}$$

with $\lambda > 0$. For each $\circ \in \{\text{KL, WKL, KW}\}$, let $P_\circ \in \text{Sym}_+(\mathbb{R}; d)$ denote the unique solution of the discrete algebraic Riccati equation (33) with the corresponding R_\circ . The optimal linear policy minimizing J° with $\gamma \in (0, 1)$ is

$$F_\circ = -\gamma (R_\circ + \gamma B^\top P_\circ B)^{-1} B^\top P_\circ A. \tag{13}$$

In particular, F_{WKL} does not depend on Σ_w . If $\Sigma_w = \rho I$ for some $\rho > 0$ and $\lambda = 1$, then

1. $\lim_{\rho \searrow 0} F_{\text{KW}} = F_{\text{WKL}}$.
2. $\lim_{\rho \rightarrow \infty} \|F_{\text{KW}} - F_{\text{KL}}\| = 0$.
3. Additionally, if the spectral radius of A is less than $\frac{1}{\sqrt{\gamma}}$, then $\lim_{\rho \searrow 0} F_{\text{KL}} = 0$ while $\lim_{\rho \searrow 0} F_{\text{KW}} = F_{\text{WKL}}$ is not the zero policy in general.

Proof. See Appendix C.1. \square

Remark 5.2. It can be shown that if A has eigen values with magnitude greater than $\frac{1}{\sqrt{\gamma}}$, then $\lim_{\rho \rightarrow 0} F_{\text{KL}}$ does not equal the zero policy. However, if $\lambda < \frac{1}{\sqrt{\gamma}}$ is an eigenvalue of A , then λ is also an eigenvalue of the closed-loop system. Thus if the open loop system has slowly decaying modes, these are not stabilized under F_{KL} yielding degraded closed-loop performance.

For a finite-horizon cost

$$\mathbb{E}_{w_t \sim \mathcal{N}(0, \Sigma_w)} \left[\sum_{t=0}^N \gamma^t (x_t^\top Q x_t + D^\circ(p_t | p_0)) \right],$$

one obtains time-varying linear state-feedback policies $u_t = F_{\circ, t} x_t$ via backwards Riccati recursions with the same effective control penalties R_\circ . Qualitatively similar behavior arises in model predictive control (MPC), where one repeatedly solves a finite-horizon divergence-regularized problem for future control inputs u_t .

5.1 Example 1: Double integrator

As a concrete example, we consider the one-dimensional double integrator system³ [48] described by

$$\begin{bmatrix} q_{t+1} \\ p_{t+1} \end{bmatrix} = \begin{bmatrix} 1 & 1 \\ 0 & 1 \end{bmatrix} \begin{bmatrix} q_t \\ p_t \end{bmatrix} + \begin{bmatrix} 0 \\ 1 \end{bmatrix} u_t + w_t,$$

where q_t is displacement, p_t is velocity, u_t is force and $w_t \sim \mathcal{N}(0, \rho I)$ with variance parameter $\rho \geq 0$. We set $Q = I$ and $\gamma = 0.9$. The assumptions of Corollary 5.1 hold.

As $\rho \searrow 0$, KL-regularization makes J^{KL} dominated by the divergence term, driving $F_{\text{KL}} \rightarrow 0$ and yielding poor closed-loop behavior. Figure 2 (and Figure 9) shows $F_{\text{KL}} \rightarrow 0$ while F_{WKL} and F_{KW} remain nonzero ; for $\lambda = 1$, KW interpolates between WKL (low noise) and KL (high noise), consistent with Corollary 5.1.

Closed-loop trajectories in Figure 3 illustrate the qualitative consequences: for small ρ , KL yields large oscillations due to vanishing feedback, whereas WKL and KW produce increasingly well-damped responses. To assess stability more directly, Figure 4 plots the spectral radius of $A + BF_\circ$ versus ρ . The KL-based closed-loop approaches the unit circle (stability boundary) as $\rho \rightarrow 0$, whereas WKL and KW avoid this pathology; KW again interpolates smoothly between the two regimes as λ varies from 1 to 0. The optimal cost are plotted in Figure 7 in the Appendix C.3 which confirming these observations further.

5.2 Example 2: Cart-pole system

We consider the cart-pole system, a standard nonlinear control benchmark and linearize it around the upright equilibrium at the origin. An LQR controller is designed using the linearized model. The resulting controller is applied to the full nonlinear dynamics to evaluate performance beyond the linear approximation (see Appendix C.2 for details). As with the double integrator, KL-regularization produces large oscillations, while WKL and KW yield increasingly stable trajectories as ρ decreases,

³A double integrator is a canonical and simplified model of a mobile robot, such as a quadrotor.

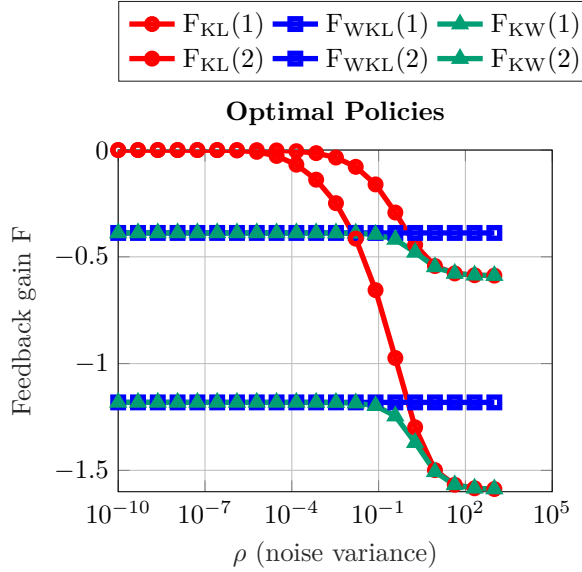


Figure 2: Optimal feedback gains for KL –, WKL –, and KW – regularized LQR as function ρ . Each feedback gain $F \in \mathbb{R}^{1 \times 2}$ shown component-wise; both entries are shown. KL gains shrink to zero as noise disappears, WKL gains are constant because they do not depend on ρ , and KW gains smoothly interpolate between the two.

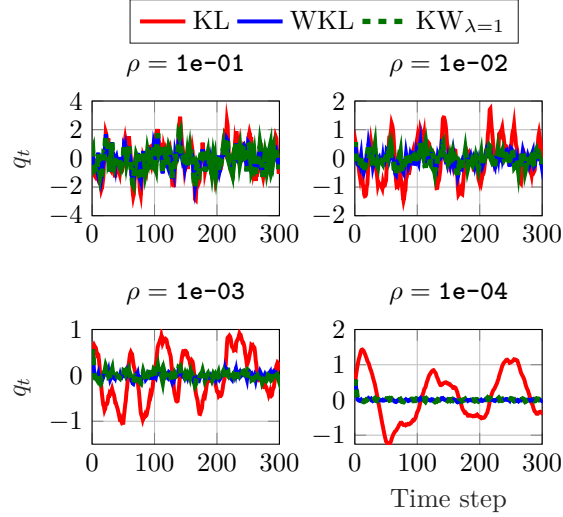


Figure 3: Closed-loop trajectories of the double integrator under KL-, WKL-, and KW-regularized controllers for $\rho \in \{10^{-1}, 10^{-2}, 10^{-3}, 10^{-4}\}$. For small ρ , KL yields weak feedback and large oscillations, whereas WKL- and KW-regularized controllers lead to reduced oscillations. See Figure 8 for other values of λ .

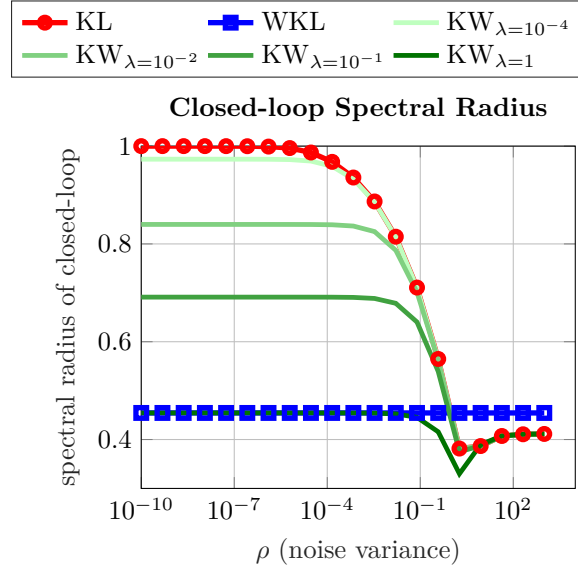


Figure 4: Closed-loop spectral radius as a function of noise ρ for different values of parameter λ . KL-regularized controllers approach the unit circle as $\rho \rightarrow 0$, indicating near-instability, while WKL- and KW-regularized controllers preserve maintain spectral radii well below one across noise regimes. Varying λ interpolates between KL-like and WKL-like behavior.

resulting in superior closed-loop performance. This is illustrated in Figure 6 which shows closed-loop trajectories of the nonlinear cart–pole under the LQR controller designed from the linearized model.

Remark 5.3 (Other regularizers). Many other divergences could be used to penalize the discrepancy between p_t and p_0 . However, even if some (like Jensen-Shannon divergence, squared Hellinger, or total variation, or maximum mean discrepancy) are bounded and thus not blow up for vanishing noise, or are explicitly modified to remain finite for measures with disjoint support [26, 53], they either admit closed forms between elliptic distributions that are not quadratic [42] or do not admit closed form expressions at all. For non-quadratic regularizers, the optimal policy F is not available in closed form.

Remark 5.4. The divergence-based regularization can be interpreted as a principled approach to selecting the control penalty matrix R in LQR design. Whereas in classical control R is typically chosen heuristically, our framework derives R_\circ from the geometry of the underlying divergence and the process noise covariance.

6 Conclusions and future work

Motivated by certain shortcomings of the KL divergences as a regularizer, we introduced state-space-aware KL divergences by considering different geometries in the dynamical formulation of the KL. These novel divergences outperform the standard KL regularizer in control problems, effortlessly, and generalize to other noise models beyond Gaussians.

Having validated our divergences in the fully tractable LQR setting, a natural next step is to integrate them into reinforcement-learning algorithms and empirically evaluate their behavior and benefits in both model-free and model-based RL. We plan to investigate new versions of the mutual information based on the divergences D^G and apply the new regularizers to different problems, for example, in imaging, and to VAEs. Further, it would be interesting to determine orbits of distributions, that is, find out which densities are reachable from another one by G -dual geodesics.

Acknowledgments. V. Stein thanks his advisor, Gabriele Steidl, for her support and guidance throughout, as well as the organizers of the *Conference on Mathematics of Machine Learning 2025* in Hamburg. Furthermore, he acknowledges fruitful conversations with Lorenz Schwachhöfer.



Funded by the European Union. Views and opinions expressed are, however, those of the author(s) only and do not necessarily reflect those of the European Union or the European Research Council Executive Agency. Neither the European Union nor the granting authority can be held responsible for them. This project has received funding from the European Research Council (ERC) under the European Union's Horizon Europe research and innovation programme (grant agreement No. 101198055, project acronym NEITALG).

References

- [1] M. Abuqrais and D. Pigoli. A Riemannian covariance for manifold-valued data. arXiv preprint arXiv:2410.06164, 2024.
- [2] F. Altekrüger, J. Hertrich, and G. Steidl. Neural Wasserstein gradient flows for discrepancies with Riesz kernels. In *Proceedings of the 40th International Conference on Machine Learning*, pages 664–690, 2023.
- [3] L. Ambrosio, N. Gigli, and G. Savaré. *Gradient flows: in metric spaces and in the space of probability measures*. Springer Science & Business Media, 2 edition, 2008.
- [4] B. D. Anderson and J. B. Moore. *Optimal control: linear quadratic methods*. Courier Corporation, 2007.
- [5] N. Ay. Information geometry of the Otto metric. *Information Geometry*, pages 1–24, 2024.
- [6] N. Ay and S.-i. Amari. A novel approach to canonical divergences within information geometry. *Entropy*, 17(12):8111–8129, 2015.
- [7] N. Ay, J. Jost, H. Ván Lê, and L. Schwachhöfer. *Information geometry*, volume 64. Springer, 2017.

- [8] N. Ay and L. J. Schwachhöfer. Torsion of α -connections on the density manifold. In *International Conference on Geometric Science of Information*, pages 417–427. Springer, 2025.
- [9] M. Bauer, M. Bruveris, and P. W. Michor. Uniqueness of the Fisher–Rao metric on the space of smooth densities. *Bulletin of the London Mathematical Society*, 48(3):499–506, 2016.
- [10] F. Beier, R. Beinert, and G. Steidl. On a linear Gromov–Wasserstein distance. *IEEE Transactions on Image Processing*, 31:7292–7305, 2022.
- [11] J.-D. Benamou and Y. Brenier. A computational fluid mechanics solution to the Monge–Kantorovich mass transfer problem. *Numerische Mathematik*, 84(3):375–393, 2000.
- [12] D. Bertsekas. *Dynamic programming and optimal control*, volume II. Belmont, MA: Athena Scientific, 3rd edition, 2011.
- [13] K. M. Borgwardt, A. Gretton, M. J. Rasch, H.-P. Kriegel, B. Schölkopf, and A. J. Smola. Integrating structured biological data by Kernel Maximum Mean Discrepancy. *Bioinformatics*, 22(14):e49–e57, 07 2006.
- [14] S. Boufadène and F.-X. Vialard. On the global convergence of Wasserstein gradient flow of the Coulomb discrepancy. *SIAM Journal on Mathematical Analysis*, 57(4):4556–4587, 2025.
- [15] J. A. Carrillo, S. Lisini, G. Savaré, and D. Slepčev. Nonlinear mobility continuity equations and generalized displacement convexity. *Journal of Functional Analysis*, 258(4):1273–1309, 2010.
- [16] M. Cuturi. Sinkhorn distances: Lightspeed computation of optimal transport. *Advances in Neural Information Processing Systems*, 26, 2013.
- [17] A. Datar and N. Ay. Wasserstein KL-divergence for Gaussian distributions. In F. Nielsen and F. Barbaresco, editors, *Geometric Science of Information*, pages 91–101, Cham, 2026. Springer Nature Switzerland.
- [18] J. Dolbeault, B. Nazaret, and G. Savaré. A new class of transport distances between measures. *Calculus of Variations and Partial Differential Equations*, 34(2):193–231, 2009.
- [19] A. Duncan, N. Nüsken, and L. Szpruch. On the geometry of Stein variational gradient descent. *Journal of Machine Learning Research*, 24(56):1–39, 2023.
- [20] R. Duong, N. Rux, V. Stein, and G. Steidl. Wasserstein gradient flows of maximum mean discrepancy functionals with distance kernels under Sobolev regularization. *Philosophical transactions. Series A, Mathematical, physical, and engineering sciences*, 383(2298):20240243, 2025.
- [21] R. Duong, V. Stein, R. Beinert, J. Hertrich, and G. Steidl. Wasserstein gradient flows of MMD functionals with distance kernel and Cauchy problems on quantile functions. *ESAIM: Control, Optimisation and Calculus of Variations*, 2026.
- [22] D. Felice and N. Ay. Towards a canonical divergence within information geometry. *Information geometry*, 4(1):65–130, 2021.
- [23] G. Frahm, M. Junker, and A. Szimayer. Elliptical copulas: applicability and limitations. *Statistics & Probability Letters*, 63(3):275–286, 2003.

- [24] T. Friedrich. Die Fisher-Information und symplektische Strukturen. *Mathematische Nachrichten*, 153(1):273–296, 1991.
- [25] A. Garbuno-Inigo, F. Hoffmann, W. Li, and A. M. Stuart. Interacting Langevin diffusions: Gradient structure and ensemble Kalman sampler. *SIAM Journal on Applied Dynamical Systems*, 19(1):412–441, 2020.
- [26] P. Glaser, M. Arbel, and A. Gretton. KALE flow: A relaxed KL gradient flow for probabilities with disjoint support. In *Advances in Neural Information Processing Systems*, volume 34, pages 8018–8031, Virtual event, 6–14 Dec 2021.
- [27] A. Gretton, K. M. Borgwardt, M. J. Rasch, B. Schölkopf, and A. Smola. A kernel two-sample test. *Journal of Machine Learning Research*, 13(25):723–773, 2012.
- [28] M. Hardion and H. Lavenant. Gradient flows of potential energies in the geometry of Sinkhorn divergences. arXiv preprint arXiv:2511.14278, 2025.
- [29] Y. Hashizume, K. Oishi, and K. Kashima. Tsallis entropy regularization for linearly solvable MDP and linear quadratic regulator. *arXiv preprint arXiv:2403.01805*, 2024.
- [30] H. J. Kappen. Path integrals and symmetry breaking for optimal control theory. *Journal of Statistical Mechanics: Theory and Experiment*, 2005(11):P11011, 2005.
- [31] V. Kučera. A review of the matrix Riccati equation. *Kybernetika*, 9(1):42–61, 1973.
- [32] S. Kullback and R. A. Leibler. On information and sufficiency. *The Annals of Mathematical Statistics*, 22(1):79–86, 1951.
- [33] J. D. Lafferty. The density manifold and configuration space quantization. *Transactions of the American Mathematical Society*, 305(2):699–741, 1988.
- [34] W. Lee, L. Wang, and W. Li. Deep JKO: time-implicit particle methods for general nonlinear gradient flows. *Journal of Computational Physics*, page 113187, 2024.
- [35] W. Li. Geometric calculations on density manifolds from reciprocal relations in hydrodynamics. arXiv preprint arXiv:2501.16479, 2025.
- [36] M. Liero and A. Mielke. Gradient structures and geodesic convexity for reaction–diffusion systems. *Philosophical Transactions of the Royal Society A: Mathematical, Physical and Engineering Sciences*, 371(2005):20120346, 2013.
- [37] Q. Liu. Stein variational gradient descent as gradient flow. *Advances in Neural Information Processing Systems*, 30, 2017.
- [38] Q. Liu and D. Wang. Stein variational gradient descent: A general purpose Bayesian inference algorithm. *Advances in Neural Information Processing Systems*, 29, 2016.
- [39] T. Liu, P. Ghosal, K. Balasubramanian, and N. Pillai. Towards understanding the dynamics of Gaussian-Stein variational gradient descent. *Advances in Neural Information Processing Systems*, 36, 2024.

- [40] A. Liutkus, U. Simsekli, S. Majewski, A. Durmus, and F.-R. Stöter. Sliced-Wasserstein flows: Nonparametric generative modeling via optimal transport and diffusions. In *International Conference on Machine Learning*, pages 4104–4113. PMLR, 2019.
- [41] J. Lott. Some geometric calculations on Wasserstein space. *Communications in Mathematical Physics*, 277(2):423–437, 2008.
- [42] F. Nielsen and K. Okamura. On the f -divergences between densities of a multivariate location or scale family. *Statistics and Computing*, 34(1), jan 2024.
- [43] N. Nüsken and D. Renger. Stein variational gradient descent: Many-particle and long-time asymptotics. *Foundations of Data Science*, 5(3):286–320, 2023.
- [44] F. Otto. The geometry of dissipative evolution equations: the porous medium equation. *Communications in Partial Differential Equations*, 26:101–174, 2001.
- [45] X. Pennec. Intrinsic statistics on Riemannian manifolds: Basic tools for geometric measurements. *Journal of Mathematical Imaging and Vision*, 25(1):127–154, 2006.
- [46] R. Peyre. Comparison between W_2 distance and \dot{H}^{-1} norm, and localization of Wasserstein distance. *ESAIM: Control, Optimisation and Calculus of Variations*, 24(4):1489–1501, 2018.
- [47] J. Rabin, G. Peyré, J. Delon, and M. Bernot. Wasserstein barycenter and its application to texture mixing. In *International Conference on Scale Space and Variational Methods in Computer Vision*, pages 435–446. Springer, 2011.
- [48] B. Recht. A tour of reinforcement learning: The view from continuous control. *Annual Review of Control, Robotics, and Autonomous Systems*, 2(1):253–279, 2019.
- [49] R. Schmidt. Tail dependence for elliptically contoured distributions. *Mathematical Methods of Operations Research*, 55(2):301–327, 2002.
- [50] J. Schulman, S. Levine, P. Abbeel, M. Jordan, and P. Moritz. Trust region policy optimization. In *International Conference on Machine Learning*, pages 1889–1897. PMLR, 2015.
- [51] V. Stein and W. Li. Towards understanding accelerated Stein variational gradient flow – analysis of generalized bilinear kernels for Gaussian target distributions. arXiv preprint arXiv:2509.04008, 2025.
- [52] V. Stein and W. Li. Accelerated Stein variational gradient flow. In F. Nielsen and F. Barbaresco, editors, *Geometric Science of Information. 7th International Conference, GSI 2025, Saint-Malo, France, October 29–31, 2025, Proceedings*, volume 16033 of *Lecture Notes in Computer Science*, pages 80–90, Cham, 2026. Springer Nature Switzerland.
- [53] V. Stein, S. Neumayer, N. Rux, and G. Steidl. Wasserstein gradient flows for Moreau envelopes of f -divergences in reproducing kernel Hilbert spaces. *Analysis and Applications*, 24(01):21–65, 2026.
- [54] J. Sun. Sensitivity analysis of the discrete-time algebraic Riccati equation. *Linear algebra and its Applications*, 275:595–615, 1998.

- [55] K. Takeda and T. Sakajo. Uniform error bounds of the ensemble transform Kalman filter for chaotic dynamics with multiplicative covariance inflation. *SIAM/ASA Journal on Uncertainty Quantification*, 12(4):1315–1335, 2024.
- [56] E. Theodorou, J. Buchli, and S. Schaal. Learning policy improvements with path integrals. In *Proceedings of the Thirteenth International Conference on Artificial Intelligence and Statistics*, pages 828–835. JMLR Workshop and Conference Proceedings, 2010.
- [57] E. Todorov. Linearly-solvable Markov decision problems. *Advances in Neural Information Processing Systems*, 19, 2006.
- [58] I. Tolstikhin, O. Bousquet, S. Gelly, and B. Schoelkopf. Wasserstein auto-encoders. arXiv preprint arXiv:1711.01558, 2017.
- [59] C. Villani. *Topics in optimal transportation*, volume 58 of *Graduate Studies in Mathematics*. American Mathematical Society, 2003.
- [60] C. Villani. *Optimal transport: old and new*, volume 338 of *Grundlehren der mathematischen Wissenschaften*. Springer Berlin, Heidelberg, 1 edition, 2008.
- [61] Y. Wang and W. Li. Accelerated information gradient flow. *Journal of Scientific Computing*, 90(1):11, 2022.
- [62] L. Xu, A. Korba, and D. Slepcev. Accurate quantization of measures via interacting particle-based optimization. In *International Conference on Machine Learning*, pages 24576–24595. PMLR, 2022.

Appendix

First, in section A, we present the proofs for section 4, which are cumbersome but straightforward, and for section B. Additionally, we define the Stein metric and compute the associated KL divergence for centered elliptic distributions. Then, in section C, we give some background on control theory and prove the related theorems mentioned in the experiments section.

A Proofs of theorems

A.1 Proof of the formula for the linearized Wasserstein KL divergence theorem 4.1

Proof. On densities, the \dot{H}^{-1} gradient flow of the potential energy $\mu \mapsto \mathbb{E}_\mu[f]$ reads $\dot{\rho}_t = -\Delta f$, so $\rho_t = \rho_0 - t\Delta f$, where ρ_0 and ρ_1 are the densities of μ and ν , respectively, with respect to the Lebesgue measure. If we let $t = 1$, then we obtain the inhomogeneous Poisson equation $-\Delta f = \rho_1 - \rho_0$, whose solution is $f = \Phi * (\rho_1 - \rho_0)$. Then, (4) becomes

$$\begin{aligned} D^{\dot{H}^{-1}}(\mu \mid \nu) &= \int_{\mathbb{R}^d} f(x) \rho_1(x) dx - \int_0^1 \int_{\mathbb{R}^d} f(x) (\rho_0(x) + t\Delta f(x)) dx dt \\ &= \int_{\mathbb{R}^d} f(x) (\rho_1(x) - \rho_0(x)) dx - \int_0^1 t \int_{\mathbb{R}^d} f(x) \Delta f(x) dx dt \\ &= \frac{3}{2} \int_{\mathbb{R}^d} f(x) (\rho_1(x) - \rho_0(x)) dx \\ &= \frac{3}{2} \int_{\mathbb{R}^d} \int_{\mathbb{R}^d} \Phi(x - y) d(\mu - \nu)(x) d(\mu - \nu)(y). \square \end{aligned}$$

A.2 Proof of lemma 4.8

Proof. 1. For the probability measures $(\mu_t)_{t \geq 0}$ associated to the densities $(\rho_t)_{t \geq 0}$, we have by [3, Lemma 8.1.4] that $\mu_t = (X_t)_{\#} \mu_0$, where the flow $(X_t: \mathbb{R}^d \rightarrow \mathbb{R}^d)_{t \geq 0}$ solves

$$\begin{cases} \dot{X}_t = v_t \circ X_t, \\ X_0 = \text{id}. \end{cases}$$

Then, there exist matrices $A_t \in \mathbb{R}^{d \times d}$ and vectors $a_t \in \mathbb{R}^d$ such that $X_t(x) = A_t x + a_t$ (where $\dot{A}_t = S_t A_t$, $A_0 = I$ and $\dot{a}_t = S_t a_t + s_t$, $a_0 = 0$). Now, suppose that $\rho_0 \sim E(m_0, \Sigma_0, g)$. Then, remark 4.4 implies for any $t > 0$ there exist $m_t \in \mathbb{R}^d$ and $\Sigma_t \in \text{Sym}_+(\mathbb{R}; d)$ such that $\rho_t \sim E(m_t, \Sigma_t, g)$.

2. We now derive the ODE (7) for the mean and covariance parameters m_t and Σ_t . Using integration by parts, we have

$$\dot{m}_t = \int_{\mathbb{R}^d} x \dot{\rho}_t(x) dx = - \int_{\mathbb{R}^d} x \nabla \cdot (\rho_t(x) v_t(x)) dx = \int_{\mathbb{R}^d} \rho_t(x) (S_t x + s_t) dx = S_t m_t + s_t,$$

and, similarly,

$$\begin{aligned}
\dot{\Sigma}_t &= \partial_t \int_{\mathbb{R}^d} (x - m_t)(x - m_t)^\top \rho_t(x) dx \\
&= \int_{\mathbb{R}^d} (x - m_t)(x - m_t)^\top \partial_t \rho_t(x) dx - 2\dot{m}_t \underbrace{\int_{\mathbb{R}^d} (x - m_t)^\top \rho_t(x) dx}_{=0} \\
&= - \int_{\mathbb{R}^d} (x - m_t)(x - m_t)^\top \nabla \cdot (v_t(x) \rho_t(x)) dx \\
&= \int_{\mathbb{R}^d} ((x - m_t)v_t(x)^\top + v_t(x)(x - m_t)^\top) \rho_t(x) dx \\
&= \int_{\mathbb{R}^d} ((x - m_t)(S_t x + s_t)^\top + (S_t x + s_t)(x - m_t)^\top) \rho_t(x) dx \\
&= \int_{\mathbb{R}^d} ((x - m_t)x^\top S_t^\top + S_t x(x - m_t)^\top) \rho_t(x) dx \\
&= \int_{\mathbb{R}^d} ((x - m_t)(x - m_t)^\top S_t^\top + S_t(x - m_t)(x - m_t)^\top) \rho_t(x) dx \\
&= \Sigma_t S_t^\top + S_t \Sigma_t. \square
\end{aligned}$$

A.3 Proof of theorem 4.10

Proof. Since $v^O(\mu, \nabla f) = \nabla f$, Lemma 4.8 gives us the linear time-invariant and decoupled system

$$\begin{cases} \dot{m}_t = B m_t + b, \\ \dot{\Sigma}_t = 2 \text{Sym}(B \Sigma_t). \end{cases} \quad (14)$$

which can be analytically solved to obtain

$$\begin{aligned} m_1 &= e^B m_0 + (e^B B^\dagger + B^\perp - B^\dagger) b, \\ \Sigma_1 &= e^B \Sigma_0 e^B. \end{aligned}$$

Under the constraints that $\Sigma_0 \succ 0$ and $\Sigma_1 \succ 0$, these equations posses a unique solution [31, Thm. 5] given by

$$B = \log \left(\Sigma_0^{-\frac{1}{2}} \left(\Sigma_0^{\frac{1}{2}} \Sigma_1 \Sigma_0^{\frac{1}{2}} \right)^{\frac{1}{2}} \Sigma_0^{-\frac{1}{2}} \right), \quad (15)$$

$$b = ((e^B - I) B^\dagger + B^\perp)^{-1} (m_1 - e^B m_0). \quad (16)$$

gives us the final result (9). \square

A.4 Proof of the Kalman-Wasserstein-KL formula in theorem 4.11

Now, we prove theorem 4.11.

Proof. 1. First, we solve the mean-covariance ODE. By eqs. (6) and (7) the geodesic $\gamma(t) \sim E(m_t, \Sigma_t, g)$ follows

$$\begin{cases} \dot{m}_t = (\kappa_g \Sigma_t + \lambda I)(B m_t + b), \\ \dot{\Sigma}_t = 2 \operatorname{Sym}((\kappa_g \Sigma_t + \lambda I)B \Sigma_t). \end{cases} \quad (17)$$

We choose B such that B and Σ_0 are simultaneously diagonalizable with

$$\Sigma_0 = Q \operatorname{diag}(s_0) Q^{-1} \quad \text{and} \quad B = Q \operatorname{diag}(\beta_i) Q^{-1}$$

From now on, we will only work in the Q -basis: we can write $\Sigma_t = Q \operatorname{diag}(s_t) Q^{-1}$, since if Σ_t is the unique solution, then $\partial_t Q^{-1} \Sigma_t Q = 2 \operatorname{Sym}((\kappa_g Q^{-1} \Sigma_t Q + \lambda I) \operatorname{diag}(\beta) Q^{-1} \Sigma_t Q)$ is diagonal. Further, let $\tilde{b} := Q^{-1}b$, and $\tilde{m}_t := Q^{-1}m_t$, we obtain

$$\begin{cases} (\dot{\tilde{m}}_t)_i = (\kappa_g(s_t)_i + \lambda)(\beta_i(\tilde{m}_t)_i + \tilde{b}_i), \\ (\dot{s}_t)_i = 2(\kappa_g(s_t)_i + \lambda)(s_t)_i \odot \beta_i, \end{cases}$$

where \odot denotes elementwise multiplication of vectors. This system can be solved componentwise: the covariance equation has the closed form solution

$$(s_i)_t = \frac{\lambda(s_0)_i}{(\kappa_g(s_0)_i + \lambda)e^{-2\lambda\beta_i t} - \kappa_g(s_0)_i}, \quad t < \begin{cases} \frac{1}{2\lambda\beta_i} \ln \left(1 + \frac{\lambda}{\kappa_g(s_0)_i} \right), & \beta_i > 0, \\ \infty, & \beta_i \leq 0. \end{cases}$$

(Equivalently, $\Sigma_t = \lambda \Sigma_0 ((\lambda I + \kappa_g \Sigma_0) e^{-2\lambda B t} - \kappa_g \Sigma_0)^{-1}$.)

Plugging this solution into the equation for the mean yields, after some algebra

$$(\tilde{m}_t)_i = \begin{cases} (\tilde{m}_0)_i + t(\kappa_g(s_0)_i + \lambda)\tilde{b}_i, & \text{if } \beta_i = 0, \\ \left((\tilde{m}_0)_i + \frac{\tilde{b}_i}{\beta_i} \right) \sqrt{\frac{\lambda}{(\kappa_g(s_0)_i + \lambda)e^{-2\lambda\beta_i t} - \kappa_g(s_0)_i}} - \frac{\tilde{b}_i}{\beta_i}, & \text{else.} \end{cases} \quad (18)$$

2. Now, we solve for B and b .

Solving for B yields

$$\begin{aligned} \Sigma_1 &= \lambda \Sigma_0 ((\lambda I + \kappa_g \Sigma_0) e^{-2\lambda B} - \kappa_g \Sigma_0)^{-1} \\ \iff e^{2\lambda B} &= (\lambda \Sigma_0^{-1} + \kappa_g I) (\lambda \Sigma_1^{-1} + \kappa_g I)^{-1}. \end{aligned}$$

Since Σ_0 and Σ_1 are symmetric positive definite matrices and $\lambda, \kappa_g > 0$, the principal matrix logarithm of the right-hand side exists and is unique, and we obtain

$$B = \frac{1}{2\lambda} \ln \left((\lambda \Sigma_0^{-1} + \kappa_g I) (\lambda \Sigma_1^{-1} + \kappa_g I)^{-1} \right).$$

The matrix B is symmetric since $\Sigma_0 \Sigma_1 = \Sigma_1 \Sigma_0$. Hence,

$$\beta_i = \frac{1}{2\lambda} \ln \left(\frac{\frac{\lambda}{(s_0)_i} + \kappa_g}{\frac{\lambda}{(s_1)_i} + \kappa_g} \right), \quad i \in \{1, \dots, d\}. \quad (19)$$

and thus $\beta_i = 0$ if and only if $(s_0)_i = (s_1)_i$ for $i \in \{1, \dots, d\}$. Hence,

$$\begin{aligned} (\Sigma_1 - \Sigma_0)^\perp &= I - (\Sigma_1 - \Sigma_0)(\Sigma_1 - \Sigma_0)^\dagger \\ &= I - Q \operatorname{diag}(s_1 - s_0) Q^{-1} Q \operatorname{diag} \left(\frac{1}{s_1 - s_0} \mathbf{1}_{s_1 \neq s_0} \right) Q^{-1} \\ &= I - Q \operatorname{diag}(1_{(s_1)_i \neq (s_0)_i}) Q^{-1} = Q \operatorname{diag}(1_{(s_1)_i = (s_0)_i}) Q^{-1}. \end{aligned}$$

Furthermore, we can solve for \tilde{b} in terms of μ and ν :

$$\tilde{b}_i = \begin{cases} \frac{(\tilde{m}_1)_i - (\tilde{m}_0)_i}{\kappa_g(s_0)_i + \lambda}, & \text{if } \beta_i = 0, \\ \beta_i \frac{(\tilde{m}_1)_i \sqrt{(\xi_1)_i} - (\tilde{m}_0)_i \sqrt{\lambda}}{\sqrt{\lambda} - \sqrt{(\xi_1)_i}}, & \text{else.} \end{cases} \quad (20)$$

where we used the shorthand $(\xi_t)_i := (\kappa_g(s_0)_i + \lambda)e^{-2\lambda\beta_i t} - \kappa_g(s_0)_i$ for $i \in \{1, \dots, d\}$. Furthermore, (19) implies

$$e^{-2\lambda\beta_i t} = \left(\frac{\frac{\lambda}{(s_1)_i} + \kappa_g}{\frac{\lambda}{(s_0)_i} + \kappa_g} \right)^t, \quad i \in \{1, \dots, d\}, \quad (21)$$

so $(\xi_1)_i = \lambda \frac{(s_0)_i}{(s_1)_i}$ for all $i \in \{1, \dots, d\}$.

3. Now, we can evaluate the divergence formula from (8):

$$D^{\text{KW}}(\mu \mid \nu) = \frac{\kappa_g}{2} \operatorname{tr}(B\Sigma_1) + \frac{1}{2} m_1^\top (Bm_1 + 2b) - \int_0^1 \frac{\kappa_g}{2} \operatorname{tr}(B\Sigma_t) + \frac{1}{2} m_t^\top (Bm_t + 2b) dt.$$

Splitting the sum into the $\beta_i = 0$ and $\beta_i \neq 0$ contributions and plugging in (18) yields

$$\begin{aligned} \frac{\kappa_g}{2} \operatorname{tr}(B\Sigma_t) + \frac{1}{2} m_t^\top (Bm_t + 2b) &= \frac{1}{2} \sum_{i=1}^d \kappa_g \beta_i (s_t)_i + (\tilde{m}_t)_i (\beta_i (\tilde{m}_t)_i + 2\tilde{b}_i) \\ &= \sum_{\substack{i=1 \\ \beta_i=0}}^d ((\tilde{m}_0)_i + t((\kappa_g s_0)_i + \lambda) \tilde{b}_i) \tilde{b}_i \\ &\quad + \frac{1}{2} \sum_{\substack{i=1 \\ \beta_i \neq 0}}^d \beta_i \underbrace{\left(\kappa_g (s_t)_i + (\tilde{m}_t)_i \left((\tilde{m}_t)_i + 2 \frac{(\tilde{m}_1)_i \sqrt{(\xi_1)_i} - (\tilde{m}_0)_i \sqrt{\lambda}}{\sqrt{\lambda} - \sqrt{(\xi_1)_i}} \right) \right)}_{=: (\star)}. \end{aligned}$$

We have

$$\begin{aligned} (\star) &= \kappa_g \frac{\lambda (s_0)_i}{\xi_t} + \left(\left((\tilde{m}_0)_i + \frac{(\tilde{m}_1)_i \sqrt{\xi_1} - (\tilde{m}_0)_i \sqrt{\lambda}}{\sqrt{\lambda} - \sqrt{\xi_1}} \right) \frac{\sqrt{\lambda}}{\sqrt{\xi_t}} - \frac{(\tilde{m}_1)_i \sqrt{\xi_1} - (\tilde{m}_0)_i \sqrt{\lambda}}{\sqrt{\lambda} - \sqrt{\xi_1}} \right) \\ &\quad \cdot \left(\left((\tilde{m}_0)_i + \frac{(\tilde{m}_1)_i \sqrt{\xi_1} - (\tilde{m}_0)_i \sqrt{\lambda}}{\sqrt{\lambda} - \sqrt{\xi_1}} \right) \frac{\sqrt{\lambda}}{\sqrt{\xi_t}} + \frac{(\tilde{m}_1)_i \sqrt{\xi_1} - (\tilde{m}_0)_i \sqrt{\lambda}}{\sqrt{\lambda} - \sqrt{\xi_1}} \right) \end{aligned}$$

$$= \kappa_g \frac{\lambda(s_0)_i}{\xi_t} + \left((\tilde{m}_0)_i + \frac{(\tilde{m}_1)_i \sqrt{\xi_1} - (\tilde{m}_0)_i \sqrt{\lambda}}{\sqrt{\lambda} - \sqrt{\xi_1}} \right)^2 \frac{\lambda}{\xi_t} - \left(\frac{(\tilde{m}_1)_i \sqrt{\xi_1} - (\tilde{m}_0)_i \sqrt{\lambda}}{\sqrt{\lambda} - \sqrt{\xi_1}} \right)^2.$$

The $\beta_i = 0$ part of $D^{\text{KW}}(\mu \mid \nu)$ is

$$\begin{aligned} & \sum_{\substack{i=1 \\ \beta_i=0}}^d \frac{(\tilde{m}_1)_i ((\tilde{m}_1)_i - (\tilde{m}_0)_i)}{\kappa_g(s_0)_i + \lambda} - \int_0^1 ((\tilde{m}_0)_i + t((\tilde{m}_1)_i - (\tilde{m}_0)_i)) dt \cdot \frac{(\tilde{m}_1)_i - (\tilde{m}_0)_i}{\kappa_g(s_0)_i + \lambda} \\ &= \sum_{\substack{i=1 \\ \beta_i=0}}^d \left((\tilde{m}_1)_i - \frac{(\tilde{m}_1)_i + (\tilde{m}_0)_i}{2} \right) \frac{(\tilde{m}_1)_i - (\tilde{m}_0)_i}{\kappa_g(s_0)_i + \lambda} = \frac{1}{2} \sum_{\substack{i=1 \\ (s_0)_i = (s_1)_i}}^d \frac{((\tilde{m}_1)_i - (\tilde{m}_0)_i)^2}{\kappa_g(s_0)_i + \lambda} \\ &= \frac{1}{2} (m_1 - m_0)^T (\Sigma_1 - \Sigma_0)^\perp (\kappa_g \Sigma_0 + \lambda I)^{-1} (\Sigma_1 - \Sigma_0)^\perp (m_1 - m_0). \end{aligned}$$

For i -th summand of the $\beta_i \neq 0$ part of $D^{\text{KW}}(\mu \mid \nu)$, we first integrate the only t -dependent term:

$$\begin{aligned} \int_0^1 \frac{1}{(\xi_t)_i} dt &= \int_0^1 \frac{1}{(\kappa_g(s_0)_i + \lambda) e^{-2\lambda\beta_i t} - \kappa_g(s_0)_i} dt \\ &= \frac{1}{\kappa_g(s_0)_i 2\lambda\beta_i} \ln \left(\frac{\lambda}{(\xi_1)_i} \right) - \frac{1}{\kappa_g(s_0)_i} \\ &= \frac{1}{2\lambda\beta_i \kappa_g(s_0)_i} \ln \left(\frac{(s_1)_i}{(s_0)_i} \right) - \frac{1}{\kappa_g(s_0)_i} \end{aligned}$$

Thus,

$$\frac{1}{(\xi_1)_i} - \int_0^1 \frac{1}{(\xi_t)_i} dt = \frac{\kappa_g(s_1)_i + \lambda}{\lambda \kappa_g(s_0)_i} - \frac{1}{2\lambda\beta_i \kappa_g(s_0)_i} \ln \left(\frac{(s_1)_i}{(s_0)_i} \right).$$

Hence, the complete contribution of each $\beta_i \neq 0$ term is (note that the affine term cancels)

$$\frac{\lambda}{2} \beta_i \left(\kappa_g(s_0)_i + \left((\tilde{m}_0)_i + \frac{(\tilde{m}_1)_i \sqrt{(\xi_1)_i} - (\tilde{m}_0)_i \sqrt{\lambda}}{\sqrt{\lambda} - \sqrt{(\xi_1)_i}} \right)^2 \right) \left(\frac{1}{(\xi_1)_i} - \int_0^1 \frac{1}{(\xi_t)_i} dt \right).$$

We have

$$(\tilde{m}_0)_i + \frac{(\tilde{m}_1)_i \sqrt{(\xi_1)_i} - (\tilde{m}_0)_i \sqrt{\lambda}}{\sqrt{\lambda} - \sqrt{(\xi_1)_i}} = \frac{\sqrt{s_0}}{\sqrt{s_1} - \sqrt{s_0}} ((\tilde{m}_1)_i - (\tilde{m}_0)_i)$$

and thus the full contribution reads

$$\begin{aligned} & \sum_{\substack{i=1 \\ (s_0)_i \neq (s_1)_i}}^d \left(\kappa_g(s_0)_i + \frac{(s_0)_i}{(\sqrt{s_1} - \sqrt{s_0})^2} ((\tilde{m}_1)_i - (\tilde{m}_0)_i)^2 \right) \left(\frac{1}{4\lambda} \ln \left(\frac{\frac{\lambda}{(s_0)_i} + \kappa_g}{\frac{\lambda}{(s_1)_i} + \kappa_g} \right) \frac{\kappa_g(s_1)_i + \lambda}{(s_0)_i \kappa_g} - \frac{1}{4\kappa_g(s_0)_i} \ln \left(\frac{(s_1)_i}{(s_0)_i} \right) \right) \\ &= \frac{1}{4\lambda} \sum_{\substack{i=1 \\ (s_0)_i \neq (s_1)_i}}^d \left(1 + \frac{((\tilde{m}_1)_i - (\tilde{m}_0)_i)^2}{\kappa_g (\sqrt{s_1} - \sqrt{s_0})^2} \right) \left(\kappa_g(s_1)_i \ln \left(\frac{(s_1)_i}{(s_0)_i} \right) + (\kappa_g(s_1)_i + \lambda) \ln \left(\frac{\lambda + \kappa_g(s_0)_i}{\lambda + \kappa_g(s_1)_i} \right) \right). \end{aligned}$$

In matrix form, we obtain

$$\frac{1}{4\lambda} \text{tr} \left((\kappa_g \Sigma_1 + \lambda I) \ln \left((\kappa_g \Sigma_0 + \lambda I) (\kappa_g \Sigma_1 + \lambda I)^{-1} \right) \right) + \frac{\kappa_g}{4\lambda} \text{tr} \left(\Sigma_1 \ln \left(\Sigma_1 \Sigma_0^{-1} \right) \right)$$

$$+ \frac{1}{4\lambda} (m_1 - m_0)^\top P \left(\Sigma_1 \ln(\Sigma_1 \Sigma_0^{-1}) + \frac{1}{\kappa_g} (\kappa_g \Sigma_1 + \lambda I) \ln((\lambda I + \kappa_g \Sigma_0)(\lambda I + \kappa_g \Sigma_1)^{-1}) \right) \\ \cdot P(\sqrt{\Sigma_1} - \sqrt{\Sigma_0})^{-2} (m_1 - m_0),$$

where $P := (\Sigma_1 - \Sigma_0)(\Sigma_1 - \Sigma_0)^\dagger$. \square

B Elementary calculations with elliptic distributions

In this section, we perform some elementary computations relating to elliptic distributions that are used in the main text.

Lemma B.1 (Covariance of elliptic distributions). *Let $X \sim \mu$ be an $E(m, \Sigma, g)$ -distributed random variable. Then, $\mathbb{E}[X] = m$ and $\mathbb{V}[X] = \frac{1}{d} \frac{\pi^{\frac{d}{2}}}{\Gamma(\frac{d}{2})} \int_0^\infty r^{\frac{d}{2}} g(r) dr \cdot \Sigma$.*

Proof. Let $Y := \Sigma^{-\frac{1}{2}}(X - m)$. Its law is $(\Sigma^{-\frac{1}{2}}(\cdot - m))_\# \mu$, whose density is $g \circ \|\cdot\|^2$. We have

$$\mathbb{E}[X] = \Sigma^{\frac{1}{2}} \underbrace{\mathbb{E}[Y]}_{=0} + m \int_{\mathbb{R}^d} g(\|y\|_2^2) dy = m \frac{\pi^{\frac{d}{2}}}{\Gamma(\frac{d}{2})} \int_0^\infty r^{\frac{d}{2}-1} g(r) dr = m,$$

where the first integral vanishes because the integrand is odd, as well as

$$\mathbb{V}[X] = \int_{\mathbb{R}^d} (x - m)(x - m)^\top p_{m, \Sigma, g}(x) dx = \Sigma^{\frac{1}{2}} \left(\int_{\mathbb{R}^d} yy^\top g(\|y\|_2^2) dy \right) \Sigma^{\frac{1}{2}}.$$

Let $\Sigma_Y := \int_{\mathbb{R}^d} yy^\top g(\|y\|_2^2) dy$. For any orthogonal matrix $O \in O(d)$, we have $O\Sigma_Y O^\top = \Sigma_Y$. Hence, there exists a $\kappa_g \in \mathbb{R}$ with $\Sigma_Y = \kappa_g \text{id}_d$. We have $\kappa_g d = \text{tr}(\Sigma_Y) = \int_{\mathbb{R}^d} \|y\|^2 g(\|y\|_2^2) dy$, so $\mathbb{V}[X] = \kappa_g \Sigma$ with

$$\kappa_g = \frac{1}{d} \int_{\mathbb{R}^d} \|y\|^2 g(\|y\|^2) dy = \frac{1}{d} \frac{\pi^{\frac{d}{2}}}{\Gamma(\frac{d}{2})} \int_0^\infty r^{\frac{d}{2}} g(r) dr. \quad \square$$

Lemma B.2 (Potential energy of elliptic distribution). *If $\mu \sim E(m, \Sigma, g)$ and $f(x) = \frac{1}{2}x^\top Bx + b^\top x + c$, then*

$$\int_{\mathbb{R}^d} f d\mu = \frac{\kappa_g}{2} \text{tr}(B\Sigma) + \frac{1}{2} m^\top Bm + b^\top m + c.$$

Proof. Using the “whitening” substitution $y := \Sigma^{-\frac{1}{2}}(x - m)$ we have

$$\begin{aligned} \int_{\mathbb{R}^d} f d\mu &= \int_{\mathbb{R}^d} \left(\frac{1}{2}x^\top Bx + b^\top x + c \right) p_{m, \Sigma, g}(x) dx \\ &= \frac{1}{2} \int_{\mathbb{R}^d} \left(m^\top + y^\top \Sigma^{\frac{1}{2}} \right) B \left(\Sigma^{\frac{1}{2}} y + m \right) g(\|y\|_2^2) dy + b^\top m + c \\ &= \frac{1}{2} \text{tr} \left(\Sigma^{\frac{1}{2}} B \Sigma^{\frac{1}{2}} \int_{\mathbb{R}^d} yy^\top g(\|y\|_2^2) dy \right) + \frac{1}{2} m^\top Bm + b^\top m + c \\ &= \frac{\kappa_g}{2} \text{tr}(B\Sigma) + \frac{1}{2} m^\top Bm + b^\top m + c, \end{aligned}$$

using that $\int_{\mathbb{R}^d} yg(\|y\|_2^2) dy = 0$, $\int_{\mathbb{R}^d} g(\|y\|_2^2) dy = 1$ and the linearity and cyclic permutation property of the trace together with $y^\top A y = \text{tr}(A y y^\top)$ and lemma B.1. \square

B.1 Calculating the vector fields for elliptic distributions

We now verify the calculations from example 4.7

Lemma B.3 (Kalman-Wasserstein vector field for elliptic distribution). *The Kalman-Wasserstein vector field for an elliptic distribution is (6).*

$$v^{\text{KW}}(p_{m,\Sigma,g}, \nabla f) = x \mapsto (\kappa_g \Sigma + \lambda \text{id}_d)(Bx + b). \quad (22)$$

Proof. Comparing (5) with (3) yields the vector field

$$v^{\text{KW}}(p_{m,\Sigma,g}, \nabla f) = \frac{m(p_{m,\Sigma,g})}{p_{m,\Sigma,g}} \nabla f = (\mathbb{V}[p_{m,\Sigma,g}] + \lambda I) \nabla f = (\kappa_g \Sigma + \lambda I_d) \nabla f. \quad \square$$

B.2 Fisher-Rao calculation

We show that

$$D^{\text{FR}}(\mu \mid \nu) = \text{KL}(\nu \mid \mu). \quad (23)$$

for $\mu, \nu \in \mathcal{P}_+^\infty(\mathbb{R}^n)$ such that

$$\int_{\mathbb{R}^n} \left| \ln \left(\frac{d\mu}{d\nu} \right) \right|^k d(\mu + \nu) < \infty, \quad k \in \{1, 2\}. \quad (24)$$

Proof. Note that the geodesic (with respect to the FR metric) is given by

$$\gamma(t) = \frac{\left(\frac{d\nu}{d\mu} \right)^t}{Z(t)} \mu = \rho_t \cdot \mu, \text{ where } Z(t) = \int_{\mathbb{R}^n} \left(\frac{d\nu}{d\mu} \right)^t d\mu.$$

Note that if $\mu = f_\mu \mathcal{L}$ and $\nu = f_\nu \mathcal{L}$, then

$$Z(t) = \int_{\mathbb{R}^n} \left(\frac{d\nu}{d\mu} \right)^t d\mu = \int_{\mathbb{R}^n} \left(\frac{f_\nu}{f_\mu} \right)^t f_\mu d\mathcal{L} = \int_{\mathbb{R}^n} \left(\frac{f_\nu}{f_\mu} \right)^t f_\mu d\mathcal{L} = \int_{\mathbb{R}^n} f_\nu^t f_\mu^{(1-t)} d\mathcal{L}.$$

Note that $f_\nu^t f_\mu^{(1-t)}$ is differentiable with respect to t and

$$\frac{d}{dt} \left(f_\nu^t f_\mu^{(1-t)} \right) = \left(f_\nu^t f_\mu^{(1-t)} \right) \ln \left(\frac{f_\nu}{f_\mu} \right).$$

The AM-GM inequality together with (24) for $k = 1$ justify differentiating under the integral sign, yielding

$$\frac{d}{dt} Z(t) = \int_{\mathbb{R}^n} \left(f_\nu^t f_\mu^{(1-t)} \right) \ln \left(\frac{f_\nu}{f_\mu} \right) d\mathcal{L} = \int_{\mathbb{R}^n} \left(\frac{f_\nu}{f_\mu} \right)^t \ln \left(\frac{f_\nu}{f_\mu} \right) d\mu = \int_{\mathbb{R}^n} \left(\frac{d\nu}{d\mu} \right)^t \ln \left(\frac{d\nu}{d\mu} \right) d\mu.$$

This gives us

$$\frac{1}{Z(t)} \frac{d}{dt} Z(t) = \frac{1}{\int_{\mathbb{R}^n} \left(\frac{d\nu}{d\mu} \right)^t d\mu} \int_{\mathbb{R}^n} \left(\frac{d\nu}{d\mu} \right)^t \ln \left(\frac{d\nu}{d\mu} \right) d\mu = \int_{\mathbb{R}^n} \ln \left(\frac{d\nu}{d\mu} \right) d\gamma(t).$$

Differentiating γ with respect to time and using the above expression for $\frac{\dot{Z}(t)}{Z(t)}$, we get that

$$\begin{aligned}\dot{\gamma}(t) &= \left(\frac{\left(\frac{d\nu}{d\mu} \right)^t \ln \left(\frac{d\nu}{d\mu} \right)}{Z(t)} - \frac{\left(\frac{d\nu}{d\mu} \right)^t \dot{Z}(t)}{Z(t)^2} \right) \mu = \left(\ln \left(\frac{d\nu}{d\mu} \right) - \frac{\dot{Z}(t)}{Z(t)} \right) \gamma(t) \\ &= \left(\ln \left(\frac{d\nu}{d\mu} \right) - \int_{\mathbb{R}^n} \ln \left(\frac{d\nu}{d\mu} \right) d\gamma(t) \right) \gamma(t) \\ &= \left(\ln \left(\frac{d\nu}{d\mu} \right) - \mathbb{E}_{\gamma(t)} \left[\ln \left(\frac{d\nu}{d\mu} \right) \right] \right) \gamma(t).\end{aligned}$$

Plugging this into the expression for D^{FR} yields

$$\begin{aligned}D^{\text{FR}}(\mu | \nu) &= \int_0^1 t \left(\int_{\mathbb{R}^n} \left(\ln \left(\frac{d\nu}{d\mu} \right) - \mathbb{E}_{\gamma(t)} \left[\ln \left(\frac{d\nu}{d\mu} \right) \right] \right)^2 d\gamma(t) \right) dt \\ &= \int_0^1 t \cdot \mathbb{E}_{\gamma(t)} \left[\left(\ln \left(\frac{d\nu}{d\mu} \right) - \mathbb{E}_{\gamma(t)} \left[\ln \left(\frac{d\nu}{d\mu} \right) \right] \right)^2 \right] dt.\end{aligned}$$

The AM-GM inequality together with (24) for $k = 2$ justify differentiating under the integral sign, yielding the standard identity

$$\frac{d}{dt} \left(\mathbb{E}_{\gamma(t)} \left[\ln \left(\frac{d\nu}{d\mu} \right) \right] \right) = \mathbb{E}_{\gamma(t)} \left[\left(\ln \left(\frac{d\nu}{d\mu} \right) - \mathbb{E}_{\gamma(t)} \left[\ln \left(\frac{d\nu}{d\mu} \right) \right] \right)^2 \right].$$

This, together with the application of integration by parts gives us

$$\begin{aligned}D^{\text{FR}}(\mu | \nu) &= \int_0^1 t \cdot \frac{d}{dt} \left(\mathbb{E}_{\gamma(t)} \left[\ln \frac{d\nu}{d\mu} \right] \right) dt \\ &= \mathbb{E}_{\gamma(1)} \left[\ln \frac{d\nu}{d\mu} \right] - \int_0^1 \left(\mathbb{E}_{\gamma(t)} \left[\ln \frac{d\nu}{d\mu} \right] \right) dt.\end{aligned}\tag{25}$$

Finally, using the fact that $\gamma(0) = \mu$ and $\gamma(1) = \nu$ and $\frac{\dot{Z}(t)}{Z(t)} = \int_{\mathbb{R}^n} \ln \left(\frac{d\nu}{d\mu} \right) d\gamma(t)$, we get that

$$\int_0^1 \left(\mathbb{E}_{\gamma(t)} \left[\ln \frac{d\nu}{d\mu} \right] \right) dt = \int_0^1 \frac{\dot{Z}(t)}{Z(t)} dt = \int_0^1 \frac{d}{dt} \ln(Z(t)) dt = \ln(Z(1)) - \ln(Z(0)) = 0,$$

which finally gives us

$$D^{\text{FR}}(\mu | \nu) = \mathbb{E}_{\nu} \left[\ln \frac{d\nu}{d\mu} \right] = \int_{\mathbb{R}^n} \ln \left(\frac{d\nu}{d\mu} \right) d\nu = \text{KL}(\nu | \mu). \square$$

B.3 The Stein metric

In this subsection, we introduce the Stein metric from SVGD and give a closed form expression for the resulting divergence D^{Stein} between two centered elliptic distributions.

Example B.4 (Stein metric). Consider a symmetric positive definite kernel $K: \mathbb{R}^d \times \mathbb{R}^d \rightarrow \mathbb{R}$, for example, a heat kernel. The *Stein isomorphism* [19, 37, 38, 43] at a density $\rho \in L^1(\mathbb{R})$ is given by

$$\varphi_{\rho \mathcal{L}}^{\text{Stein}}([f]) := -\operatorname{div} \left(\rho \int_{\mathbb{R}^d} K(\cdot, y) \operatorname{grad}(f)(y) \rho(y) dy \right) \mathcal{L}.$$

The associated inner product on the cotangent space is

$$\langle\langle [f], [g] \rangle\rangle_{\rho \mathcal{L}}^{\text{Stein}} := \int_{\mathbb{R}^d} \int_{\mathbb{R}^d} K(x, y) \nabla f(x)^\top \nabla g(y) \rho(x) \rho(y) dx dy.$$

By considering density-dependent kernels, one can also construct a “normalized Stein metric” [62]. •

From now on, we focus on the kernel $K(x, y) := x^\top A y + a$ for the Stein metric, where $A \in \operatorname{Sym}_+(\mathbb{R}; d)$ and $a \geq 0$. We choose this kernel because its simple structure facilitates closure in the family of elliptical distribution for other (accelerated) gradient flows [1, 39, 52].

Lemma B.5 (Stein vector field with generalized bilinear kernel and elliptic distribution). *Let $\mu \sim E(m, \Sigma, g)$ and $\nabla f(x) = Bx + b$. Then, for $x \in \mathbb{R}^d$ we have*

$$v^{\text{Stein}}(\mu, f)(x) = \int_{\mathbb{R}^d} x^\top A y (By + b) p_{m, \Sigma, g}(y) dy = (B(\kappa_g \Sigma + mm^\top) + bm^\top) Ax. \quad (26)$$

Proof. For an $E(m, \Sigma, g)$ -distributed random variable X , the integral can be expressed as

$$\mathbb{E}[(x^\top A X)(BX + b)] = (B \mathbb{E}[XX^\top] + b \mathbb{E}[X]^\top) Ax$$

By lemma B.1, $\mathbb{E}[X] = m$ and

$$\mathbb{E}[XX^\top] = \mathbb{V}[X] + mm^\top = \kappa_g \Sigma + mm^\top,$$

so that

$$\int_{\mathbb{R}^d} x^\top A y (By + b) p_{m, \Sigma, g}(y) dy = (B(\kappa_g \Sigma + mm^\top) + bm^\top) Ax. \quad \square$$

Remark B.6. Recall that the KL between two Gaussians is

$$\frac{1}{2} \left[\Delta m^\top \Sigma_1^{-1} \Delta m - \operatorname{tr}(\Sigma_1^{-1} \Delta \Sigma) + \ln \left(\frac{\det(\Sigma_1)}{\det(\Sigma_0)} \right) \right]. \quad (27)$$

The Stein divergence with bilinear kernel between elliptic distributions corresponds to a “pre-conditioned” (reverse) KL divergence (compare with (27)), so for this simple kernel, we do not get “state-space-awareness”.

Theorem B.7 (Stein divergence with bilinear kernel). *Suppose $\mu \sim E(0, \Sigma_0, g)$ and $\nu \sim E(0, \Sigma_1, g)$, $K(x, y) = x^\top A y + a$, and Σ_0, Σ_1 and A all commute. Then with $R = \Sigma_1 \Sigma_0^{-1}$ we have*

$$D^{\text{Stein}}(\mu \mid \nu) = \frac{1}{4} \operatorname{tr}(A^{-1}(R - I_d - \log(R))).$$

In particular, if $A = I_d$, then $D^{\text{Stein}}(\mu \mid \nu) = \frac{1}{2} \operatorname{KL}(\nu \mid \mu)$.

Proof. Setting $b = 0$ in (7) and plugging in the Stein vector field (26) yields

$$\begin{cases} \dot{m}_t = B(\kappa_g \Sigma_t + m_t m_t^\top) A m_t, \\ \dot{\Sigma}_t = 2 \text{Sym}(\Sigma_t B(\kappa_g \Sigma_t + m_t m_t^\top) A). \end{cases}$$

First, $m_0 = m_1 = 0$ implies that $\dot{m}_t = m_t = 0$, so we only have to focus on the covariance equation.

Since A , Σ_0 , Σ_1 are simultaneously diagonalizable, we can work in this basis to reduce this ODE system to

$$\dot{\sigma}_i(t) = 2b_i \kappa_g \sigma_i(t)^2 a_i.$$

where for $i \in \{1, \dots, d\}$ and $t \geq 0$, $a_i > 0$, $\sigma_i(t) > 0$, and β_i are the eigenvalues of A , Σ_t and B , respectively. The solution is given by

$$\sigma_i(t) = \frac{1}{\sigma_i(0)^{-1} - 2\kappa_g a_i \beta_i t}, \quad i \in \{1, \dots, d\}.$$

Solving for β_i in terms of the boundary conditions yields

$$\beta_i = \frac{1}{2\kappa_g a_i} (\sigma_i(0)^{-1} - \sigma_i(1)^{-1}), \quad i \in \{1, \dots, d\},$$

which can be written in matrix form as

$$B = \frac{1}{2\kappa_g} A^{-1} (\Sigma_0^{-1} - \Sigma_1^{-1})$$

This also shows a posteriori that the solution for σ_i exists on $[0, 1]$, so everything is well-defined. By (9),

$$\begin{aligned} D^{\text{Stein}}(\mu \mid \nu) &= \frac{\kappa_g}{2} \left(\text{tr}(B \Sigma_1) - \int_0^1 \text{tr}(B \Sigma_t) dt \right) = \frac{\kappa_g}{2} \sum_{i=1}^d \beta_i \left(\sigma_i(1) - \int_0^1 \sigma_i(t) dt \right) \\ &= \sum_{i=1}^d \frac{1}{4a_i} \left(\frac{\sigma_i(1)}{\sigma_i(0)} - 1 - \ln \left(\frac{\sigma_i(1)}{\sigma_i(0)} \right) \right). \square \end{aligned}$$

We leave the exploration of the Stein divergence for different kernels for future work.

C Linear Quadratic Optimal Control with Discounted Cost

This appendix provides a concise, self-contained statement and proof of the Bellman optimality equation along with its solution for the discounted infinite-horizon linear-quadratic regulator problem.

Let the (measurable) state space be $\mathcal{X} \subseteq \mathbb{R}^n$ and the (measurable) action space be $\mathcal{U} \subseteq \mathbb{R}^m$. We consider controlled Markov dynamics

$$x_{k+1} = f(x_k, u_k, w_k), \quad (28)$$

where w_k are i.i.d. random disturbances (on a probability space $(\Omega, \mathcal{F}, \mathbb{P})$), and the initial state x_0 satisfies $\mathbb{E}[x_0] = \mu_0$ and $\mathbb{E}[(x_0 - \mu_0)(x_0 - \mu_0)^\top] = \Sigma_0$. A memory-less (static) policy $\pi = (\pi_0, \pi_1, \dots)$ is a sequence of measurable maps $\pi_k : \mathcal{X} \rightarrow \mathcal{U}$ and the discounted cost under policy π is

$$J(\pi) := \mathbb{E} \left[\sum_{k=0}^{\infty} \gamma^k \ell(x_k, u_k) \right], \quad (29)$$

where $\ell : \mathcal{X} \times \mathcal{U} \rightarrow [0, \infty)$ is the stage cost, $u_k = \pi_k(x_k)$ and $\gamma \in (0, 1)$ is the discount factor. For a given policy π , define the value function V^π as

$$V^\pi(x) := \mathbb{E} \left[\sum_{k=0}^{\infty} \gamma^k \ell(x_k, u_k) \mid x_0 = x \right] \quad (30)$$

and the optimal value function

$$V^*(x) := \inf_{\pi} V^\pi(x), \quad x \in \mathcal{X}. \quad (31)$$

Note that

$$J(\pi) = \mathbb{E} \left[\sum_{k=0}^{\infty} \gamma^k \ell(x_k, u_k) \right] = \mathbb{E} \left[\mathbb{E} \left[\sum_{k=0}^{\infty} \gamma^k \ell(x_k, u_k) \mid x_0 \right] \right] = \mathbb{E} [V^\pi(x_0)].$$

We assume the standard discounted LQR conditions: (A, B) is stabilizable and $(A, Q^{1/2})$ is detectable, ensuring existence and uniqueness of optimal linear feedback policies for the cost defined below [4]. The following result is classical in dynamic programming and optimal control; see, for example, [12].⁴ We include a self-contained proof here, both to fix notation and because the result in the precise form and setting used in this paper is not readily available in the literature.

Theorem C.1. *Let $\mathcal{X} = \mathbb{R}^n$, $\mathcal{U} = \mathbb{R}^m$ and consider the problem of minimizing $J(\pi)$ given in (29) with quadratic stage cost*

$$\ell(x, u) = \frac{1}{2} (x^\top Q x + u^\top R u), \quad Q \succeq 0, \quad R \succ 0,$$

discount factor $\gamma \in (0, 1)$ and linear Markovian dynamics

$$x_{k+1} = Ax_k + Bu_k + w_k$$

where $A \in \mathbb{R}^{n \times n}$ and $B \in \mathbb{R}^{n \times m}$. Assume that the initial state x_0 and the exogenous disturbances w_k satisfy the following statistical properties:

1. $\mathbb{E}[x_0] = \mu_0$ and $\mathbb{E}[(x_0 - \mu_0)(x_0 - \mu_0)^\top] = \Sigma_0$ for $\Sigma_0 \succeq 0$ and
2. w_k are i.i.d. with $\mathbb{E}[w_k] = 0$ and $\mathbb{E}[w_k w_k^\top] = \Sigma_w$ for $\Sigma_w \succeq 0$.

⁴See also the expository blog post by Stephen Tu for an intuitive derivation: <https://stephentu.github.io/blog/control-theory/optimal-control/2017/12/09/discounted-infinite-horizon-lqr.html>.

Consider the value function V^π under a given policy π as defined in (30) and the optimal value function V^* as defined in (31). Assume that the pair (A, B) is stabilizable and $(A, Q^{1/2})$ is detectable. Then the optimal value function V^* satisfies the Bellman equation

$$V^*(x) = \inf_{u \in \mathcal{U}} \left\{ \ell(x, u) + \gamma \mathbb{E}[V^*(x_1) \mid x_0 = x, u_0 = u] \right\}, \quad x \in \mathcal{X}. \quad (32)$$

Furthermore, the quadratic optimal value function $V^*(x) = \frac{1}{2} \left(x^\top P x + \frac{\gamma}{1-\gamma} \text{Trace}(P \Sigma_w) \right)$ satisfies the Bellman equation (32) where P is the unique positive semi-definite solution to the algebraic Riccati equation

$$A_\gamma^\top P A_\gamma - P + Q - A_\gamma^\top P B (B^\top P B + R_\gamma)^{-1} B^\top P A_\gamma = 0, \quad (33)$$

where $A_\gamma = \sqrt{\gamma} A$ and $R_\gamma = \frac{1}{\gamma} R$. The optimal cost is given by

$$J^* = J(\pi^*) = \inf_{\pi} J(\pi) = E[V^*(x_0)]$$

and the the optimal policy π^* (time-invariant) is given by $\pi^* = (\pi_F, \pi_F, \dots)$ with $\pi_F : \mathbb{R}^n \ni x \mapsto u = Fx \in \mathbb{R}^m$ where $F = -(R + \gamma B^\top P B)^{-1} \gamma B^\top P A$.

Proof. Let us first note that the stabilizability of (A, B) implies that there exists a matrix $F \in \mathbb{R}^{m \times n}$ such that the matrix $(A + BF)$ is Schur. This means that there exists a linear time-invariant policy $\pi = (\pi_F, \pi_F, \dots)$ with $\pi_F : \mathbb{R}^n \ni x_k \mapsto u_k = Fx_k \in \mathbb{R}^m$ for all k , such that $V^\pi(x) < \infty$ for any $x \in \mathbb{R}^n$. Thus, the optimization problem is well-defined.

By using the tower property of conditional expectation when conditioning on x_1 , we get that for any policy $\pi = (\pi_0, \pi_1, \pi_2, \dots)$,

$$\begin{aligned} V^\pi(x) &= \mathbb{E} \left[\sum_{k=0}^{\infty} \gamma^k \ell(x_k, u_k) \mid x_0 = x \right] = \ell(x, \pi_0(x)) + \gamma \mathbb{E} \left[\sum_{k=0}^{\infty} \gamma^k \ell(x_{k+1}, u_{k+1}) \mid x_0 = x \right] \\ &= \ell(x, \pi_0(x)) + \gamma \mathbb{E} \left[\mathbb{E} \left[\sum_{k=0}^{\infty} \gamma^k \ell(x_{k+1}, u_{k+1}) \mid x_1 \right] \mid x_0 = x \right] \\ &= \ell(x, \pi_0(x)) + \gamma \mathbb{E}[V^{\pi^+}(x_1) \mid x_0 = x], \end{aligned} \quad (34)$$

where $\pi^+ = (\pi_1, \pi_2, \pi_3, \dots)$. We now prove the Bellman equation (32) by showing

$$\inf_{u \in \mathcal{U}} \{ \ell(x, u) + \gamma \mathbb{E}[V^*(x_1) \mid x_0 = x, u_0 = u] \} \geq V^*(x) \geq \inf_{u \in \mathcal{U}} \{ \ell(x, u) + \gamma \mathbb{E}[V^*(x_1) \mid x_0 = x, u_0 = u] \}. \quad (35)$$

Using (34) and the fact that $V^* \leq V^\pi$ pointwise for any π , we get that

$$V^\pi(x) = \ell(x, \pi_0(x)) + \gamma \mathbb{E}[V^{\pi^+}(x_1) \mid x_0 = x] \geq \ell(x, \pi_0(x)) + \gamma \mathbb{E}[V^*(x_1) \mid x_0 = x].$$

Taking the infimum over all policies (equivalently over the first-stage action $u = \pi_0(x)$ on the RHS) yields the lower bound

$$V^*(x) \geq \inf_{u \in \mathcal{U}} \{ \ell(x, u) + \gamma \mathbb{E}[V^*(x_1) \mid x_0 = x, u_0 = u] \}. \quad (36)$$

We now prove the upper bound of V^* in (35). By the definition of $V^*(x)$, we get that for any $x \in \mathcal{X}$ and any $\varepsilon > 0$, there exists a policy $\pi^{\varepsilon,x}$ such that

$$V^{\pi^{\varepsilon,x}}(x) \leq V^*(x) + \varepsilon.$$

We can now construct a new causal policy $\pi^\varepsilon = (\pi_0^\varepsilon, \pi_1^\varepsilon, \pi_2^\varepsilon, \dots)$, where $\pi_0^\varepsilon : \mathcal{X} \rightarrow \mathcal{U}$ is an arbitrary map and $(\pi_1^\varepsilon, \pi_2^\varepsilon, \dots) = \pi^{\varepsilon,x_1}$ which depends on the realization x_1 . Using (34), we get that

$$\begin{aligned} V^*(x) &\leq V^{\pi^\varepsilon}(x) = \ell(x, \pi_0^\varepsilon(x)) + \gamma \mathbb{E}[V^{(\pi^\varepsilon)^+}(x_1) \mid x_0 = x] \\ &= \ell(x, \pi_0^\varepsilon(x)) + \gamma \mathbb{E}[V^{\pi^{\varepsilon,x_1}}(x_1) \mid x_0 = x] \\ &\leq \ell(x, \pi_0^\varepsilon(x)) + \gamma \mathbb{E}[V^*(x_1) \mid x_0 = x] + \gamma \varepsilon. \end{aligned}$$

Since the above inequality holds for any map π_0^ε and arbitrary $\varepsilon > 0$, we can optimize over maps π_0^ε (effectively over $u \in \mathcal{U}$) and take the limit as ε goes to 0 to obtain

$$V^*(x) \leq \inf_{u \in \mathcal{U}} (\ell(x, u) + \gamma \mathbb{E}[V^*(x_1) \mid x_0 = x, u_0 = u]). \quad (37)$$

This completes the proof of (35), which proves (32).

We now plug in the quadratic form of $V^* = \frac{1}{2}(x^\top Px + c)$, along with the quadratic form of the stage cost ℓ as well as the expression for x_1 obtained from the system dynamics (28) into the Bellman equation (32) to get

$$x^\top Px + c = \inf_{u \in \mathcal{U}} \left(\begin{bmatrix} x^\top & u^\top \end{bmatrix} \begin{bmatrix} \gamma A^\top PA + Q & \gamma A^\top PB \\ \gamma B^\top PA & \gamma B^\top PB + R \end{bmatrix} \begin{bmatrix} x \\ u \end{bmatrix} \right) + \gamma \text{Trace}(P\Sigma_w) + \gamma c \quad (38)$$

The optimization problem over \mathcal{U} can be solved to obtain the optimal $u^* = \underbrace{-(R + \gamma B^\top PB)^{-1} \gamma B^\top PA x}_{F}$ which gives us the optimal policy π^* such that $V^{\pi^*} = V^*$. Plugging this back into equation (38) gives the Riccati equation (33) and $c = \frac{\gamma}{1-\gamma} \text{Trace}(P\Sigma_w)$. Under stabilizability and detectability assumptions, the Riccati equation has a unique positive semi-definite solution [4]. Finally, note that $J(\pi) = \mathbb{E}[V^\pi(x_0)]$. Since $V^\pi(x) \geq V^*(x)$ for any x and for any π , we get that $\inf_\pi J(\pi) = \inf_\pi \mathbb{E}[V^\pi(x_0)] \geq \mathbb{E}[V^*(x_0)]$. On the other hand, since there exists a policy π^* such that $V^{\pi^*} = V^*$, we get that $\mathbb{E}[V^*(x_0)] = \mathbb{E}[V^{\pi^*}(x_0)] \geq \inf_\pi \mathbb{E}[V^\pi(x_0)] = \inf_\pi J(\pi)$. This shows that $\inf_\pi J(\pi) = \mathbb{E}[V^*(x_0)]$. □

C.1 Proof of corollary 5.1

Proof. First note that since B has full column rank, $R_\circ \succ 0$ for $\circ \in \{\text{KL, WKL, KW}\}$. The first part of the statement is a straightforward application of Theorem C.1. Now assume $\Sigma_w = \rho I$ and $\lambda = 1$. With this choice, we get that,

$$\begin{aligned} R_{\text{KW}} &= \frac{1}{\rho+1} B^\top B \rightarrow B^\top B = R_{\text{WKL}} && \text{as } \rho \rightarrow 0 \quad \text{and} \\ \|R_{\text{KW}} - R_{\text{KL}}\| &= \frac{1}{\rho(\rho+1)} \|B^\top B\| \rightarrow 0 && \text{as } \rho \rightarrow \infty. \end{aligned}$$

Using the perturbation analysis of DARE (see [54]), we get the limiting situations 1. and 2. Finally, if the spectral radius of A is less than $\frac{1}{\sqrt{\gamma}}$, then the spectral radius of $A_\gamma = \sqrt{\gamma}A$ is less than 1. This implies that the Lyapunov equation

$$A_\gamma^\top P A_\gamma - P + Q = 0 \quad (39)$$

has a positive definite solution. Since R_{KL} grows unbounded as $\rho \rightarrow 0$, the term $(B^\top P_{KL} B + R_\gamma)^{-1}$ approaches 0 and the solution of the Riccati equation (33) converges to the solution of the Lyapunov equation (39), and thus remains bounded. Therefore, the optimal gain F_{KL} given by (13) converges to 0 as $\rho \rightarrow 0$. This completes the proof. \square

C.2 Results on the cart-pole system

C.2.1 Cart-pole model, linearization and discretization

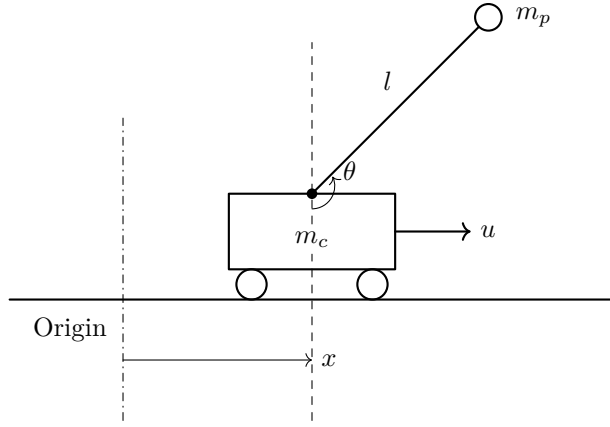


Figure 5: Cart-pole system

The cart-pole system is depicted in Figure 5. The equations of motion are given by

$$\begin{aligned} (m_c + m_p)\ddot{x} + m_p l \ddot{\theta} \cos(\theta) - m_p l \dot{\theta}^2 \sin(\theta) &= u, \\ m_p l \ddot{x} \cos(\theta) + m_p l^2 \ddot{\theta} + m_p g l \sin(\theta) &= 0 \end{aligned}$$

where x is the cart horizontal position, θ is the pendulum angle, m_c is the cart mass, m_p is the pendulum mass, l is the pendulum length (distance from the pivot to the pendulum center of mass), g is the coefficient of gravity, and u is the horizontal force applied to the cart. Introducing the generalized coordinate $q = [x \ \dot{x} \ \theta \ \dot{\theta}]$, the dynamics can be written compactly as

$$\frac{dq}{dt} = f(q, u).$$

Consider a forced equilibrium (q^*, u^*) such that $f(q^*, u^*) = 0$. Using the linear approximation of f around this equilibrium, the non-linear system can be linearized to obtain an approximate linear

time-invariant system in deviation variables $\tilde{q} = q - q^*$ as

$$\frac{d\tilde{q}}{dt} = \frac{dq}{dt} = f(q, u) \approx \underbrace{f(q^*, u^*)}_{0} + \underbrace{\frac{\partial f}{\partial q}(q^*, u^*)}_{A_c} \underbrace{(q - q^*)}_{\tilde{q}} + \underbrace{\frac{\partial f}{\partial u}(q^*, u^*)}_{B_c} \underbrace{(u - u^*)}_{\tilde{u}} = A_c \tilde{q} + B_c \tilde{u}.$$

For the upright equilibrium $q^* = [0 \ 0 \ \pi \ 0]$ and $u^* = 0$, we get

$$A_c = \begin{bmatrix} 0 & 1 & 0 & 0 \\ 0 & 0 & \frac{m_p g}{m_c} & 0 \\ 0 & 0 & 0 & 1 \\ 0 & 0 & \frac{(m_c + m_p)g}{lm_c} & 0 \end{bmatrix}, \quad B_c = \begin{bmatrix} 0 \\ 1 \\ \frac{m_c}{0} \\ \frac{1}{lm_c} \end{bmatrix}.$$

Finally, we discretize the linearized continuous-time system with sampling time T_s using a zero-order-hold scheme to obtain the discrete-time system

$$\tilde{q}_{k+1} = \underbrace{e^{A_c T_s}}_A \tilde{q}_k + \underbrace{\int_0^{T_s} e^{A_c \tau} B_c d\tau}_{B} \tilde{u}_k = A \tilde{q}_k + B \tilde{u}. \quad (40)$$

This discrete-time linear system (A, B) is then used as input to the LQR design.

C.2.2 Simulation results with the Cart-pole system

Figure 6 shows the cart position trajectories for the nonlinear cart-pole system. As with the double integrator, KL-regularization produces large oscillations, while WKL and KW yield increasingly stable trajectories as ρ decreases, resulting in superior closed-loop performance.

C.3 Optimal cost

Figure 7 shows the optimal costs with different regularizers, supporting the observations of Section 5.1

C.4 Effects of varying λ

Figure 8 and Figure 9 supplement the Figure 3 and Figure 2, respectively, and plot additional trajectories with different values of λ .

C.5 Comparison of Divergence balls

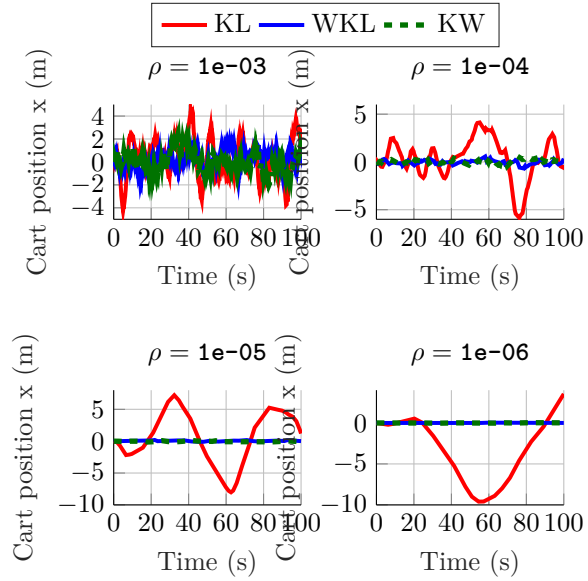


Figure 6: Closed-loop cart positions for the nonlinear cart–pole under KL-, WKL-, and KW-regularized controllers for $\rho \in \{10^{-3}, 10^{-4}, 10^{-5}, 10^{-6}\}$. At low noise, KL produces near-zero feedback and large oscillations, whereas WKL and KW reduce oscillations.

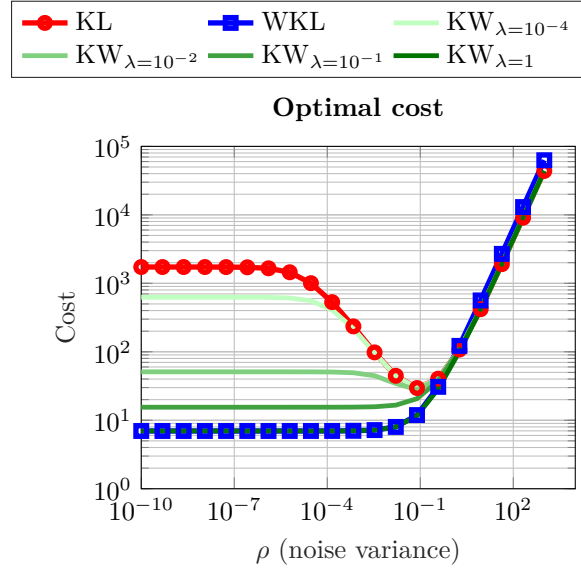


Figure 7: Optimal costs J° as a function of noise ρ for $\lambda \in \{10^{-4}, 10^{-2}, 10^{-1}, 1\}$

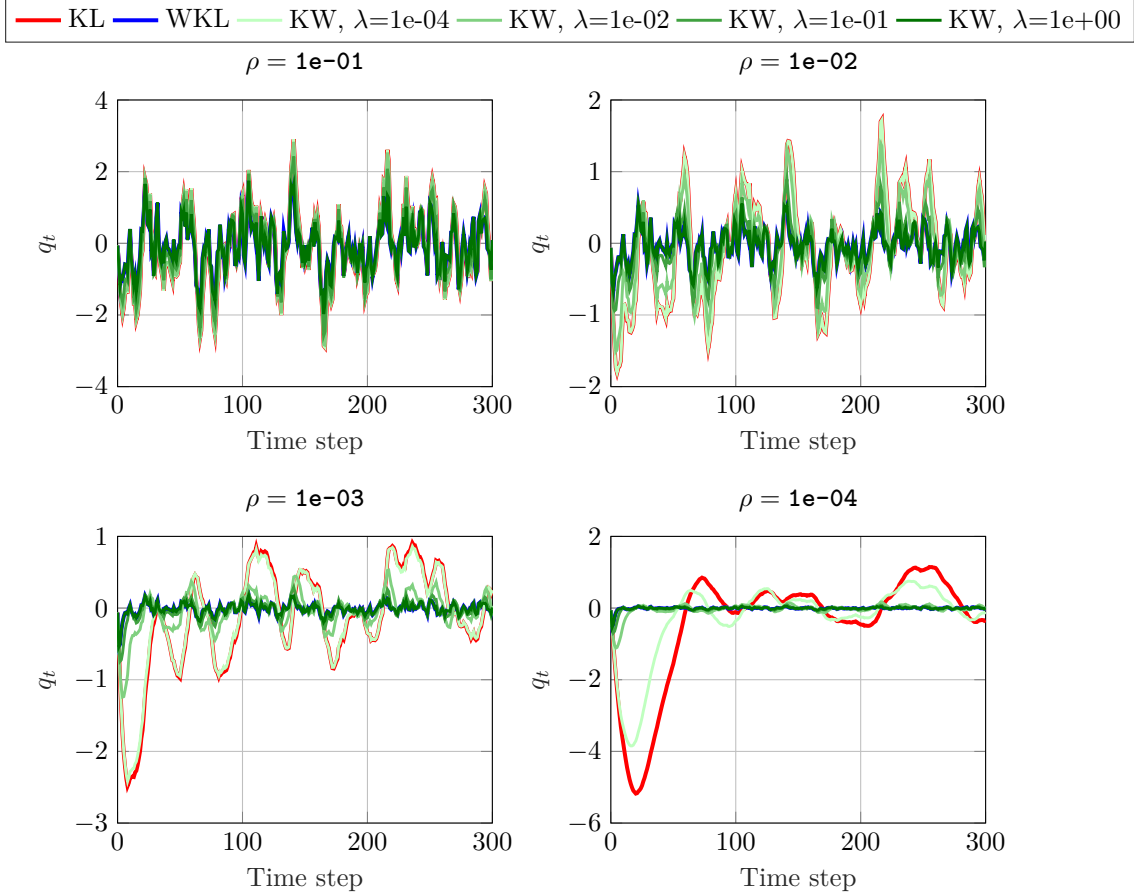


Figure 8: Closed-loop trajectories of the double integrator under KL-, WKL-, and KW-regularized controllers for noise levels $\rho \in \{10^{-1}, 10^{-2}, 10^{-3}, 10^{-4}\}$. At low noise, KL produces near-zero feedback and large oscillations, whereas WKL and KW yield more stable trajectories. For KW, varying the parameter λ interpolates smoothly between KL-like and WKL-like behavior.

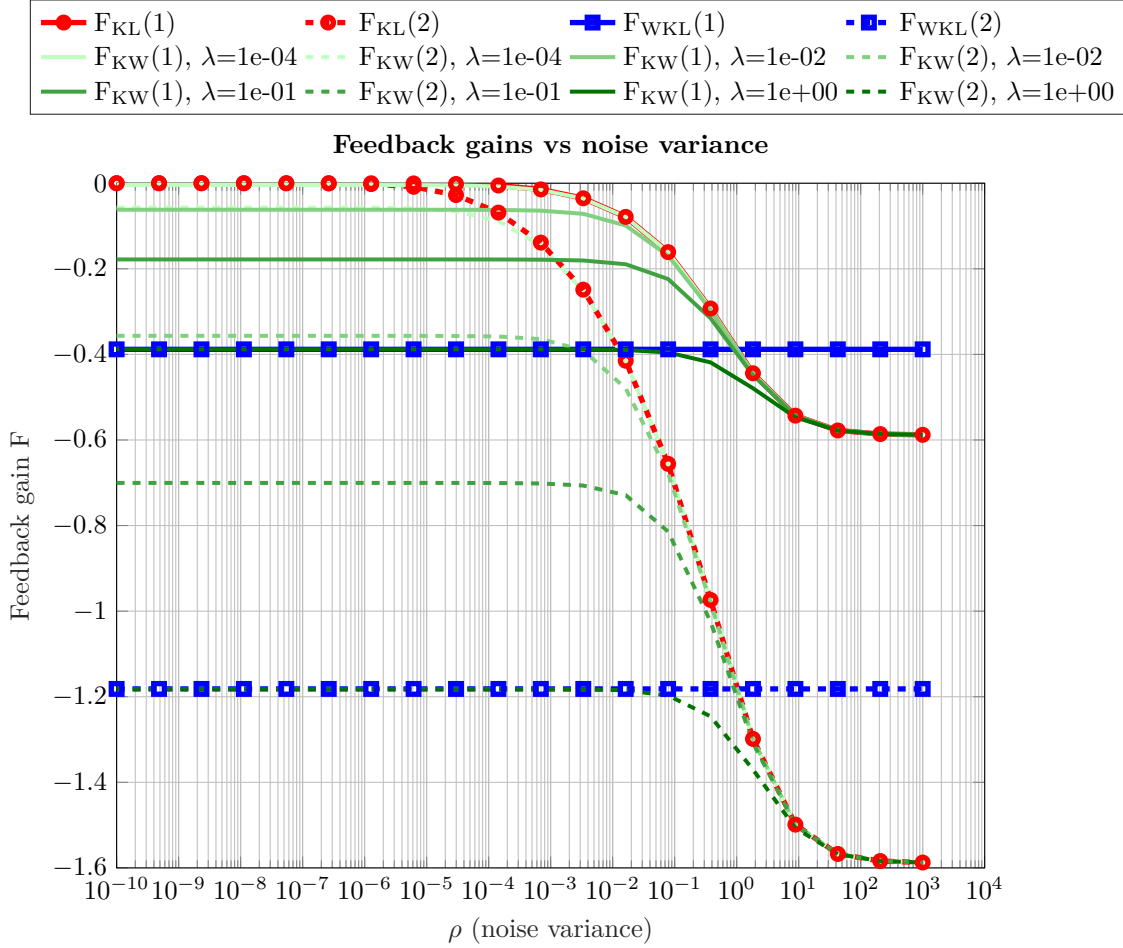


Figure 9: Comparison of optimal policies for $\{\text{KL, WKL, KW}\}$ -regularized LQR. Each linear policy is represented by a 1×2 gain matrix F ; both entries are shown. KL gains shrink to zero as noise disappears, WKL gains remain constant since they do not depend on ρ , and KW gains smoothly interpolate between the two.

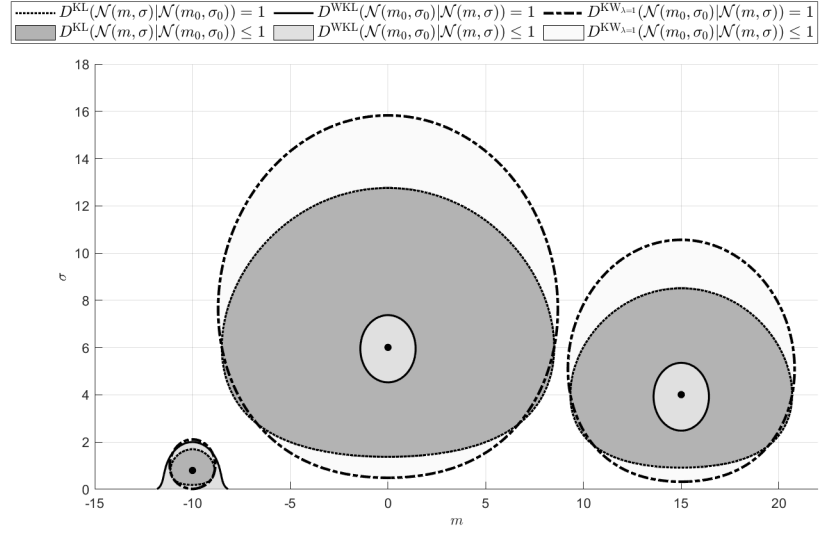


Figure 10: Comparison of sub-level sets for KL-divergence, WKL-divergence, and KWKL-divergence centered at various univariate Gaussian reference distributions $\mathcal{N}(m_0, \sigma_0)$, indicated by solid markers. Each shaded region represents the set of distributions $\mathcal{N}(m, \sigma)$ whose divergence from the reference is less than or equal to 1.

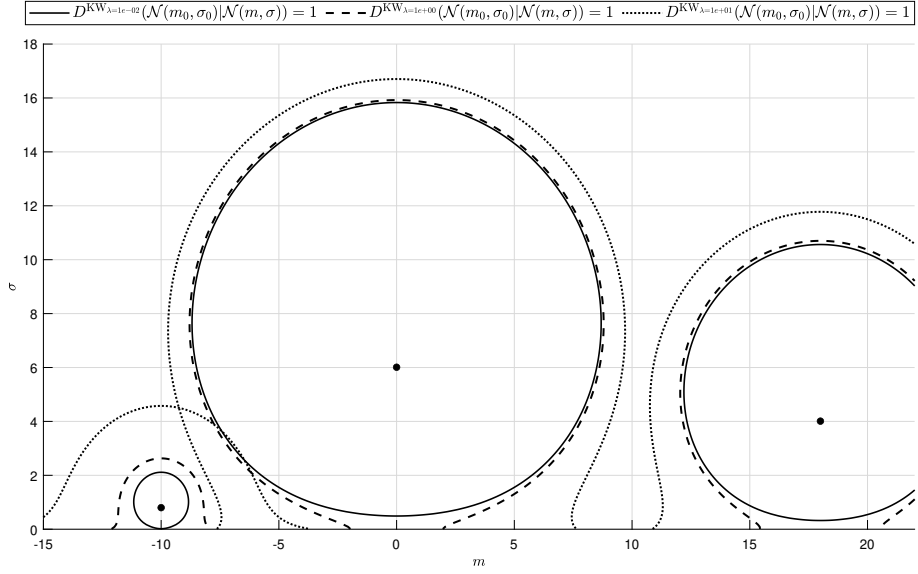


Figure 11: Level sets for KWKL-divergence centered at various univariate Gaussian reference distributions $\mathcal{N}(m_0, \sigma_0)$, indicated by solid markers for different values of λ .